



Contents lists available at ScienceDirect

Atmospheric Environment

journal homepage: www.elsevier.com/locate/atmosenv

Estimating North American background ozone in U.S. surface air with two independent global models: Variability, uncertainties, and recommendations

A.M. Fiore^{a,*}, J.T. Oberman^c, M.Y. Lin^d, L. Zhang^{e,f}, O.E. Clifton^a, D.J. Jacob^e, V. Naik^g, L.W. Horowitz^d, J.P. Pinto^h, G.P. Milly^b

^a Department of Earth and Environmental Sciences Columbia University, 61 Route 9W, Palisades, NY 10964, USA

^b Lamont-Doherty Earth Observatory of Columbia University, 61 Route 9W, Palisades, NY, USA

^c Nelson Institute Center for Sustainability and the Global Environment (SAGE), University of Wisconsin-Madison, Madison, WI, USA

^d NOAA Geophysical Fluid Dynamics Laboratory and Atmospheric and Oceanic Sciences, Princeton University, 201 Forrestal Road, Princeton, NJ, USA

^e School of Engineering and Applied Sciences, Harvard University, 29 Oxford Street, Cambridge, MA, USA

^f Department of Atmospheric and Oceanic Sciences & Laboratory for Climate and Ocean-Atmosphere Studies, School of Physics, Peking University, China

^g UCAR/NOAA Geophysical Fluid Dynamics Laboratory, Princeton, NJ, USA

^h U.S. EPA, National Center for Environmental Assessment, Research Triangle Park, NC, USA

H I G H L I G H T S

- North American Background (NAB) surface O₃ provided by two independent global models.
- Models often bracket observations implying, value in multi-model approach.
- NAB is highest at high-altitude sites in spring where it correlates with total O₃.
- NAB is lowest over the Eastern U.S. in summer where it generally does not correlate with total O₃.
- Largest model differences in NAB due to stratosphere, wildfires, lightning, isoprene.

A R T I C L E I N F O

Article history:

Received 26 December 2013

Received in revised form

24 July 2014

Accepted 26 July 2014

Available online 30 July 2014

Keywords:

Surface ozone

Background ozone

Air pollution

Air quality

Exceptional events

A B S T R A C T

Accurate estimates for North American background (NAB) ozone (O₃) in surface air over the United States are needed for setting and implementing an attainable national O₃ standard. These estimates rely on simulations with atmospheric chemistry-transport models that set North American anthropogenic emissions to zero, and to date have relied heavily on one global model. We examine NAB estimates for spring and summer 2006 with two independent global models (GEOS-Chem and GFDL AM3). We evaluate the base simulations, which include North American anthropogenic emissions, with mid-tropospheric O₃ retrieved from space and ground-level O₃ measurements. The models often bracket the observed values, implying value in developing a multi-model approach to estimate NAB O₃. Consistent with earlier studies, the models robustly simulate the largest nation-wide NAB levels at high-altitude western U.S. sites (seasonal average maximum daily 8-h values of ~40–50 ppb in spring and ~25–40 ppb in summer) where it correlates with observed O₃. At these sites, a 27-year GFDL AM3 simulation simulates observed O₃ events above 60 ppb and indicates that year-to-year variations in NAB O₃ influence their annual frequency (with NAB contributing 50–60 ppb or more during individual events). During summer over the eastern United States (EUS), when photochemical production from regional anthropogenic emissions peaks, NAB is largely uncorrelated with observed values and it is lower than at high-altitude sites (average values of ~20–30 ppb). Four processes contribute substantially to model differences in specific regions and seasons: lightning NO_x, biogenic isoprene emissions and chemistry, wildfires, and stratosphere-to-troposphere transport. Differences in the representations of these processes within the GFDL AM3 and GEOS-Chem models contribute more to uncertainty in NAB estimates, particularly in spring when NAB is highest, than the choice of horizontal resolution within a single model.

* Corresponding author.

E-mail addresses: amfiore@ldeo.columbia.edu (A.M. Fiore), oberman.wisc@gmail.com (J.T. Oberman), meiyun.lin@noaa.gov (M.Y. Lin), zhanglg@pku.edu.cn (L. Zhang), oclifton@ldeo.columbia.edu (O.E. Clifton), djacob@fas.harvard.edu (D.J. Jacob), Vaishali.Naik@noaa.gov (V. Naik), larry.horowitz@noaa.gov (L.W. Horowitz), Pinto.Joseph@epa.gov (J.P. Pinto), gpm2109@columbia.edu (G.P. Milly).

(GEOS-Chem). We propose that future efforts seek to constrain these processes with targeted analysis of multi-model simulations evaluated with observations of O₃ and related species from multiple platforms, and thereby reduce the error on NAB estimates needed for air quality planning.

© 2014 Elsevier Ltd. All rights reserved.

1. Introduction

The United States Environmental Protection Agency (U.S. EPA) sets National Ambient Air Quality Standards (NAAQS) to protect human health and welfare. Under the Clean Air Act, ground-level ozone (O₃) is regulated as a criteria air pollutant, reviewed every five years to assess and incorporate the best available scientific evidence. Following these reviews, the level for the O₃ NAAQS has been lowered over the past decade, from 0.08 ppm in 1997 to the current level of 0.075 ppm (75 ppb) in 2008, with proposals calling for even lower levels, within a range of 60–70 ppb on the basis of the latest health evidence (Federal Register, 2010). A location is considered to be in violation of the O₃ NAAQS when the three-year-average of the fourth highest daily maximum 8-h average O₃ (MDA8) exceeds the current 75 ppb level. In order to better understand how the O₃ NAAQS can be attained most effectively, a fundamental, quantitative understanding of the background O₃ – both its magnitude and variability– over the United States is needed.

The first draft of the current U.S. EPA Policy Assessment (EPA, 2013) and McDonald-Buller et al. (2011) describe the relevance of background O₃ in the U.S. national O₃ standard-setting process. Here we review recent model estimates for background O₃ (Table 1) and compare simulations from two independent models (GEOS-Chem and GFDL AM3) in the context of observational constraints with a focus on spatial, seasonal, and daily variability. Differences between the models provide a first estimate of the error in our quantitative understanding. A process-oriented multi-model approach, tied closely to *in situ* and space-based observations, can harness the strengths of individual models to provide information requested by air quality managers during both the standard-setting and implementation processes.

The term “background” is ambiguous, with several definitions used in practice to estimate it from observations and models (e.g., see discussion in Fiore et al., 2003). In the context of a review of the NAAQS, it is useful to define background O₃ concentrations in a way that distinguishes the O₃ produced from precursor emissions that are relatively less controllable versus from precursor emissions that are relatively more controllable through U.S. policies. The U.S. EPA thus defines a North American Background (NAB) as the O₃ levels that would exist in the absence of continental North American (i.e., Canadian, U.S., and Mexican) anthropogenic emissions (EPA, 2006). NAB includes contributions from natural sources (stratospheric intrusions), emissions of precursors from natural sources (e.g., wildfires, lightning, biogenic) throughout the globe, anthropogenic methane (CH₄), and emissions of anthropogenic pollutants from countries outside North America that contribute to global O₃ abundances. This definition restricts NAB to a model construct, estimated in simulations in which North American anthropogenic emissions are set to zero. The desire to quantify the impact of Canadian and Mexican emissions on NAB O₃ has led to the term “U.S. background”, a parallel model construct but estimated by setting only U.S. anthropogenic emissions to zero.

The development of effective State Implementation Plans (SIPs), by which states demonstrate how non-attainment regions will reach compliance with the NAAQS, requires an accurate assessment of the role of local, regional, and background sources in

contributing to individual high-O₃ events. The Clean Air Act includes a provision for ‘exceptional events’, whereby high-O₃ events due to natural causes (such as wildfires or stratospheric intrusions) or foreign influence (e.g., Asian pollution) can be exempted from counting towards non-attainment status (Federal Register, 2007). Modeling the individual components of NAB can provide information to aid in attributing such events to specific sources.

In the previous review cycle (EPA, 2006) of the O₃ NAAQS, the Air Quality Criteria Document considered NAB estimates from the GEOS-Chem model for a single year (Fiore et al., 2003), the only estimates documented in the published literature at that time. Recent work has updated those estimates (Wang et al., 2009; Zhang et al., 2011), compared them with NAB in regional models using GEOS-Chem boundary conditions (Emery et al., 2012; Mueller and Mallard, 2011) and considered additional years. The first NAB estimates with an independent global model, (GFDL AM3; hereafter AM3; Table 2) were found to episodically reach 60–75 ppb over the Western United States in spring (Lin et al., 2012a). By contrast, GEOS-Chem estimated a maximum NAB of 65 ppb (Zhang et al., 2011) and the AM3 NAB was typically ~10 ppb higher than GEOS-Chem NAB on days when observations exceeded 70 ppb (Lin et al., 2012a). Lin et al. (2012a, 2012b) are discussed in the Integrated Science Assessment (ISA) for the current O₃ NAAQS review cycle (EPA, 2013) but they focused on a different simulation year (2010) from the other studies. The ISA supplemental material does include a comparison of GEOS-Chem and GFDL AM3 for the same year (2006) at a measurement site in Gothic, CO, U.S.A. Here we extend that initial analysis by examining, in a consistent and process-oriented manner, the AM3 and GEOS-Chem NAB estimates during March through August of 2006. We additionally draw on a multi-decadal AM3 simulation to provide context for the single year inter-comparison. We include an evaluation of total surface O₃ in the base simulations with ground-based and space-based observations during 2006 to identify conclusions that are robust to the specific modeling system, as well as situations where observation-based constraints can be most effective in reducing uncertainty.

2. Review of prior model estimates for NAB and its components

We focus here on model estimates for NAB using the U.S. EPA definition, which relies on simulations with North American anthropogenic emissions set to zero. Earlier reviews synthesize observations relevant for evaluating base model simulations at remote sites (McDonald-Buller et al., 2011; Reid et al., 2008; Vingarzan, 2004). Even with the same approach, model estimates will differ due to different representations of natural emissions and the choice of different years since meteorological variability alters the balance between transported versus regionally produced O₃. In Table 1, we summarize published model estimates of various statistics for NAB, along with estimates from individual NAB sources (wildfires, lightning, the stratosphere, global anthropogenic CH₄ plus international anthropogenic emissions, and the sum of all natural sources).

Despite quantitative differences, a basic consensus emerges that the highest NAB levels generally occur during springtime and over western U.S. (WUS) high-altitude regions, with lowest NAB levels

Table 1

Model estimates for North American Background (NAB) ozone using the current U.S. EPA definition (North American anthropogenic emissions set to zero) and for specific components of NAB (ppb).

Study model	Study period; metric	NAB	Components
Fiore et al. (2003); GC ($2^\circ \times 2.5^\circ$)	Mar–Oct 2001; 1–5 pm mean	Typically 15–35; up to 40–50 (highest in spring and WUS)	<i>Natural</i> : 18–23 (NW), 18–27 (SW), 13–20 (NE), 15–21 (SE) <i>Strat</i> : always <10 <i>CH₄+intercontinental transport (ICT)</i> : 5–12
Wu et al. (2008); GC with winds from GISS GCM ($4^\circ \times 5^\circ$)	2000 Climatology; 1–5 pm mean	12–30 (summer); 22–40 (April); highest in WUS	<i>Natural</i> : 10–15 (EUS, summer); 15–25 (WUS, summer)
Wang et al. (2009); GC ($1^\circ \times 1^\circ$)	Summer 2001; MDA8	26 ± 8 USB: 30 ± 8; up to 33 ppb during events	
Zhang et al. (2011); GC ($\frac{1}{2}^\circ \times \frac{2}{3}^\circ$)	Mar–Aug 2006–2008; MDA8	39–44 (spring); 35–45 (summer); low-alt 27 ± 8; high-alt 40 ± 7; 51–59 (4th highest)	<i>Natural</i> : 18 ± 6 (low-alt); 27 ± 6 (high-alt); 34–45 (4th highest). <i>CH₄+ICT</i> : 13–16 (spring) 11–13 (summer); 13 (high alt); 9 (low alt)
Emery et al. (2012); CAMx (12 km ²), GC boundary conditions	Mar–Aug 2006; MDA8	25–50 ppb (20–45 in GC); 35–100 (4th highest; 65 max without fires; 55 max in GC)	<i>Fires</i> : 10–50 ppb (events)
Lin et al. (2012a); GFDL AM3 (~50 km ²)	Apr–Jun 2010; MDA8	15 WUS high-alt sites: 50 ± 11 (mean); 55 ± 11 (days when obs exceed 60 ppb)	<i>Strat</i> : 15 WUS high-alt sites: 22 ± 12 (mean); 15–25 for obs O ₃ @ 60–70; 17–40 for obs O ₃ @ 70–85 <i>Median, bias-corrected</i> : 10–22 (W); 8–13 (NE); 3–8 (SE) <i>Max, bias-corrected</i> : 35–55 (W); 30–45 (EUS)
McKeen et al. (2002); 3D regional model (60 km ²)	Jun–Jul 1995; 1–4 pm mean		<i>Fires</i> : 10–30 ppb (event, Central and EUS)
Collins et al. (2003); STOCHEM driven by UM HadAM4 GCM)	March 1991–1994 monthly mean		<i>Strat</i> : 5–15 ppb (highest in WUS)
Kaynak et al. (2008); CMAQ (36 km ²)	Jul–Aug 2004; MDA8		<i>Lightning</i> : up to 10 ppb; 14 ppb 4th highest; <2 ppb 71% of the time
Mueller and Mallard (2011); CMAQ, GC boundary conditions (36 km ²)	2002; MDA8		<i>Fires</i> : 30–50 (WUS, events) <i>Lightning</i> : 10–30 (Southern US, events)
Zhang et al. (2014); GC ($\frac{1}{2}^\circ \times \frac{2}{3}^\circ$)	Mar–Aug 2006; MDA8		<i>Lightning</i> : 6–10 ppbv (summer); <i>Fires</i> : ~20 (local events), 1–3 (WUS summer mean); <i>Strat</i> : 8–10 (WUS spring mean), up to 15 (events)

over EUS low-altitude regions in summer. The summertime minimum reflects the peak in regional photochemistry, which leads to accumulation of O₃ generated from regional precursors at the same time as it shortens the lifetime of O₃ mixing downward into the photochemically active boundary layer (see e.g., Fiore et al., 2002). At high-altitude WUS sites, models consistently indicate a day-to-day correlation between NAB levels and total O₃ during spring (Emery et al., 2012; Fiore et al., 2003; Lin et al., 2012a, 2012b; Zhang et al., 2011), implying that enhanced NAB levels play a role in raising total O₃, including above the level of the NAAQS. While these results are qualitatively consistent across several modeling platforms, the models vary in their quantitative attributions for NAB and its specific sources.

A few studies report the annual fourth highest MDA8 NAB value, the metric used to assess compliance with the O₃ NAAQS. Consideration of different metrics and different years complicates using the ranges across different modeling systems in Table 1 as error estimates. For example, mean values of NAB are unlikely to be static from year to year due to trends and variability in global anthropogenic emissions of O₃ precursors, in natural sources of NAB, and in the dominant regional transport patterns (Lin et al., 2014). A multi-model parameterization indicates an increase of ~4 ppb between 1960 and 2000 due to rising global CH₄ plus international anthropogenic emissions of non-CH₄ O₃ precursors (Wild et al., 2012). More recent increases in Asian emissions may have

additionally raised WUS NAB by up to 3 ppb in spring between 2001 and 2006 (Zhang et al., 2008). The Asian, European, and global anthropogenic CH₄ components of NAB have received particular attention under the UNECE Task Force on Hemispheric Transport of Air Pollution (Fiore et al., 2009; Reidmiller et al., 2009; TFHTAP, 2010; Wild et al., 2012). Recent studies have documented the mechanisms by which Asian pollution can reach surface air over the WUS (e.g., Brown-Steiner and Hess, 2011; Lin et al., 2012b).

Wang et al. (2009) additionally estimated summertime U.S. Background (USB), which includes the influence of Canadian and Mexican anthropogenic emissions (but not CH₄) for 2001 conditions. They found that average USB is 4 ppb higher than NAB over the contiguous United States, and up to 33 ppb higher during transport events at U.S. border sites directly downwind of these sources. In the model, Canadian and Mexican sources often contributed more than 10 ppb to total surface O₃ in excess of the 75 ppb NAAQS level in eastern Michigan, western New York, New Jersey, and southern California (Wang et al., 2009).

The natural portion of NAB has been quantified in a few modeling studies and generally follows the same patterns as total NAB, with maximum levels occurring during spring at high-altitude regions of the WUS (Table 1). Natural sources of NAB can also contribute to high-O₃ events. Observational evidence indicates events mainly of stratospheric origin at high-altitude sites in the WUS (e.g., Langford et al., 2009) but these efforts are hampered by a

Table 2
GFDL AM3 and GEOS-Chem model configurations.

Model	GFDL AM3 (Donner et al., 2011) (Rasmussen et al., 2012) (Naik et al., 2013) (Lin et al., 2012b)	GEOS-Chem http://acmg.seas.harvard.edu/geos/ (Zhang et al., 2011) (Bey et al., 2001) (Park et al., 2004)
Grid	Cubed sphere with 48×48 cell faces, approximately $2^\circ \times 2^\circ$ horizontal resolution. Vertical coordinate is a 48-level hybrid sigma grid, with the top level at 0.01 hPa; lowest 5 layers extend to 60, 130, 220, 330, and 470 m for surface pressure of 1013.25 hPa and scale height of 7.5 km.	Continental North American nested (Wang et al., 2004) simulation at $\frac{1}{2}^\circ$ latitude by $\frac{2}{3}^\circ$ longitude using boundary conditions from boundary conditions from a $2^\circ \times 2.5^\circ$ global simulation. Vertical grid has 47 levels to 0.01 hPa, with lowest 5 layers centered at 70, 200, 330, 470, 600 m for a column at sea level.
Meteorology	Online, nudged to NCEP u and v (Kalnay et al., 1996). The nudging timescale is inversely proportional to pressure (Lin et al., 2012b)	Assimilated from NASA GEOS-5
Stratospheric ozone	Stratospheric chemistry and dynamics seamlessly coupled to the troposphere (Naik et al., 2013)	Linoz parameterization (McLinden et al., 2000)
Isoprene nitrate yield and fate	Observationally-constrained 8% yield with 40% NO_x recycling (Horowitz et al., 2007 and references therein)	18% yield with no NO_x recycling (permanent sink for NO_x)
Lightning NO_x distribution	Parameterized based on convective cloud top height (Price and Rind, 1992), and described in Horowitz et al. (2003); global source in 2006 is 4.9 Tg N a^{-1} ; range over 1981–2007 is $4.4\text{--}4.9 \text{ Tg N a}^{-1}$.	Scaled to match a top-down global constraint of 6 Tg N a^{-1} (Martin et al., 2007) and spatially redistributed based on the LIS/OTD flash climatology (Murray et al., 2012) and includes a yield of $500 \text{ mol N flash}^{-1}$ at northern mid-latitudes and $125 \text{ mol N flash}^{-1}$ elsewhere (Hudman et al., 2007)
Anthropogenic emissions	ACCMIP (Lamarque et al., 2010) with annual interpolation after 2000 to RCP4.5 2010 value (Lamarque et al., 2011). NO_x emissions are 27 (global), 5.6 (North America ^a), 5.9 (East Asia ^b) Tg N a^{-1} . CO are 640 (global), 100 (North America), 160 (East Asia) Tg CO a^{-1} . C_3H_8^c are 2.9 (global), 0.3 (North America), 0.5 (East Asia) Tg C a^{-1} .	EDGAR (Olivier and Berdowski, 2001) with U.S. emissions from 2005 National Emissions Inventory (NEI-05). NO_x emissions are 27.9 (global), 6.4 (North America ^a), 7.9 (East Asia ^b) Tg N a^{-1} . CO are 582 (global), 91 (North America), 192 (East Asia) Tg CO a^{-1} . C_3H_8^c are 27 (global), 0.45 (North America), 4.1 (East Asia) Tg C a^{-1} .
Biogenic emissions	Model of Emissions of Gases and Aerosols from Nature (MEGAN) 2.1 (Guenther et al., 2006), implemented as described by Emmons et al. (2010) and Rasmussen et al. (2012). Emissions are 385 (global) and 32 (North America) Tg C a^{-1} .	MEGAN 2.0 (Guenther et al., 2006) Emissions are 404 (global) and 30 (North America) Tg C a^{-1} .
Biomass burning emissions	As for anthropogenic emissions but distributed vertically as recommended by Dentener et al. (2006). NO_x emissions are 5.3 (global), 0.18 (North America ^a), 0.14 (East Asia ^b) Tg N a^{-1} . CO are 440 (global), 18 (North America), 14 (East Asia) Tg CO a^{-1} . C_3H_8^c are 1.5 (global), 0.09 (North America), 0.09 (East Asia) Tg C a^{-1} .	GFEDv2 year-specific monthly fires (van der Werf et al., 2006), emitted at the surface. NO_x emissions are 5.1 (global), 0.14 (North America ^a), 0.12 (East Asia ^b) Tg N a^{-1} . CO are 410 (global), 12 (North America), 11 (East Asia) Tg CO a^{-1} . C_3H_8^c are 1.7 (global), 0.05 (North America), 0.06 (East Asia) Tg C a^{-1} .

^a North American domain is $15\text{--}55^\circ\text{N}$ and $60\text{--}125^\circ\text{W}$.

^b East Asian domain is $15\text{--}50^\circ\text{N}$, $95\text{--}160^\circ\text{E}$.

^c C_3H_8 is provided as an example non- CH_4 volatile organic compound (NMVOC).

sparse observational network. Models are useful for quantifying the frequency of these events and for determining the contribution of these events to seasonal mean O_3 levels. For decades, quantifying the stratospheric contribution to the troposphere, and particularly to surface air, has been contentious, with controversy rooted in the imprecise methods for quantifying accurately this component, as summarized in Lin et al. (2012a) (see their Section 2.3). Lin et al. (2012a) demonstrate that stratospheric intrusions play an important role in driving variability, including high- O_3 events, at high-altitude WUS sites during spring. High-altitude greatly increases susceptibility to stratospheric influence; for days when observed O_3 exceeds 70 ppb at monitoring sites in the Intermountain West during April–June of 2010, Lin et al. (2012a) find that median values of stratospheric O_3 in the AM3 model are 10 ppb lower at the lower elevation sites than at high-elevation sites. Episodic wildfires have also been shown to contribute to high- O_3 events (e.g., Jaffe and Wigder, 2012; McKeen et al., 2002; Mueller and Mallard, 2011), though Singh et al. (2010) found little O_3 production in wildfire plumes over California unless mixing with an urban plume occurred.

3. North American background estimates from two independent global models

We compare background estimates for March through August of 2006 from two independent global models: the GEOS-Chem global chemistry-transport model (CTM) and the GFDL AM3 chemistry-climate model nudged to re-analysis winds. The models include different representations of the processes contributing to the abundance and distributions of tropospheric O_3 (Table 2). We

evaluate the base O_3 simulations with hourly measurements from a ground-based network of monitoring sites and with monthly averaged retrievals from satellite instruments that are sensitive to O_3 in the mid-troposphere. We compare the models for March through August of 2006, the period analyzed previously by Zhang et al. (2011), drawing on a 27-year AM3 simulation to place the 2006 NAB estimates in the context of inter-annual variability. We note that the inter-annual variability may be underestimated in AM3 over some regions due its use of climatological inventories for soil NO_x and wildfire emissions.

3.1. Model simulations, observations and analysis methods

Table 2 describes the GEOS-Chem and AM3 model configurations for the base simulations (meteorological year 2006). The GEOS-Chem CTM has been applied in various configurations over the past decade to estimate NAB and its various components for the summer of 1995 (Fiore et al., 2002), the 2001 O_3 season (Fiore et al., 2003; Wang et al., 2009), and the 2006–2008 O_3 seasons (Zhang et al., 2011, 2014) including evaluation with *in situ* and satellite observations. The AM3 model has previously been applied at $\sim 50 \text{ km}$ horizontal resolution globally to estimate the impacts of Asian pollution and stratospheric intrusions on surface O_3 over the WUS from March through June of 2010; evaluation with *in situ* and space-based observations for that period shows it represents the subsidence of Asian and stratospheric O_3 plumes over the WUS (Lin et al., 2012a, 2012b). The AM3 simulation used here is $\sim 200 \text{ km}$ horizontal resolution and is multi-decadal (1980–2007; first year is discarded as initialization), enabling us to place the year 2006 in the context of inter-annual variability (Table 2 and Section 4). Both

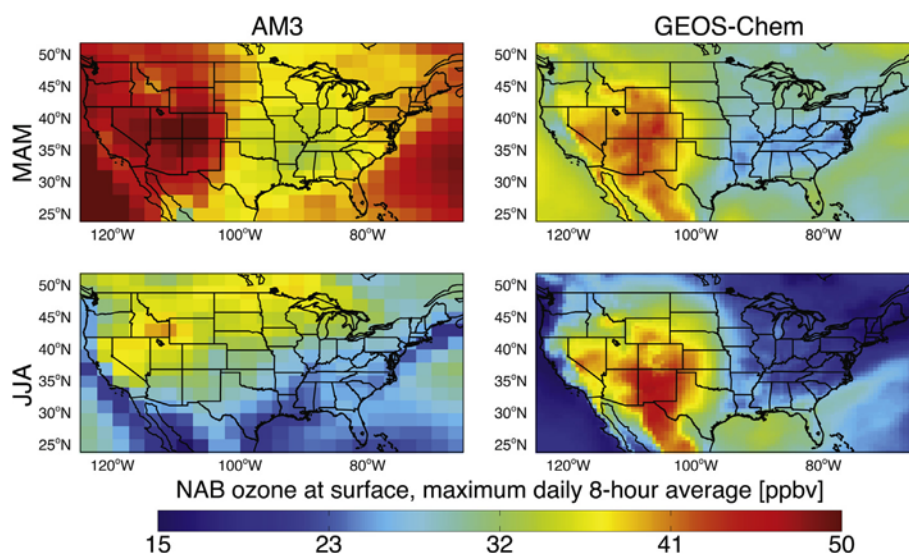


Fig. 1. Mean MDA8 values of North American Background (NAB) in the lowest model layer for the GFDL AM3 (left; $\sim 2^\circ \times 2^\circ$ horizontal resolution) and GEOS-Chem (right; $\frac{1}{2}^\circ \times \frac{2}{3}^\circ$) simulations for spring (MAM; top row) and summer (JJA; bottom row) of 2006. NAB is estimated with simulations in which North American anthropogenic emissions are set to zero. See Table 1 for model configurations.

models estimate NAB in U.S. surface air by setting North American anthropogenic emissions of aerosol and O_3 precursors to zero. Anthropogenic sources include fossil and biofuel combustion (including aircraft and ship emissions within the domain), agricultural waste burning, and fertilizer application.

For anthropogenic emissions inventories, GEOS-Chem uses the 2005 National Emissions Inventory for the U.S., while AM3 uses the historical Atmospheric Chemistry–Climate Model Intercomparison Project (ACCMIP) emissions developed in support of the IPCC AR5 (Lamarque et al., 2011, 2010). Global, North American, and East Asian annual emissions for 2006 are provided in Table 2. Differences in the North American anthropogenic emissions inventories (5.58 and 6.67 Tg N a^{-1} in AM3 and GEOS-Chem, respectively; 4.85 and 5.32 Tg N a^{-1} for the United States), while crucial to the standard simulation for comparison with observations, should be irrelevant for the NAB simulations. Shortcomings in model representation of anthropogenic emissions or isoprene chemistry do not necessarily imply shortcomings in the NAB simulations, which may still be useful for quantifying daily to inter-annual variability driven by the transported components of NAB, such as O_3 associated with stratospheric intrusions, production from lightning NO_x , wildfires, or CH_4 .

The ground-based U.S. EPA Clean Air Status and Trends Network (CASTNet) sites were situated in order to provide regionally representative measurements and to minimize the influence of polluted urban air (Baumgardner et al., 2002) and thus are useful for evaluating O_3 simulated by coarse grid models. Our evaluation focuses on MDA8 O_3 concentrations, the statistic currently used by the U.S. EPA to assess compliance with the O_3 NAAQS, at 77 CASTNet sites. Simulated MDA8 is calculated from archived hourly average O_3 concentrations in the model surface layer. The models use a terrain-following sigma-coordinate for near-surface layers, with the lowest layer centered at approximately 60 m and 70 m for a column where the lowest layer is at sea level in GFDL AM3 and GEOS-Chem, respectively. All statistics are calculated by sampling the models at the locations of CASTNet sites with bilinear interpolation from the four nearest model grid cells to the latitude and longitude at each station.

Columns retrieved from satellite instruments are sensitive to free tropospheric O_3 and enable an evaluation on a continuous

spatial scale of the simulated background available to subside into surface air. We use here direct tropospheric O_3 retrievals from both the Ozone Monitoring Instrument (OMI) (Liu et al., 2010) and the Tropospheric Emission Spectrometer (TES) (Beer, 2006). All data are processed using a single fixed a priori profile as described in Zhang et al. (2010). Previous validation of these retrievals against *in situ* and aircraft measurements indicate an accuracy to within 5 ppb at 500 hPa (Zhang et al., 2010 and references therein). Annual biases averaged over 2005–2007 relative to northern mid-latitude O_3 sondes (Zhang et al., 2010) have been uniformly subtracted from the retrieved products prior to evaluating the AM3 and GEOS-Chem base simulations. As evident from Zhang et al. (2010) (see their Fig. 5), the bias is not uniform and thus the real model error may deviate at any particular location from the true O_3 abundance differently than implied by the comparison with the satellite products reported here. We apply the appropriate satellite averaging kernels to the model daily O_3 fields for direct comparison with the retrieved satellite O_3 columns (Zhang et al., 2010). While the averaging kernels for the 500 hPa retrieved product for both the TES and OMI instruments are most sensitive to the mid-troposphere, there is a broad vertical sensitivity throughout the troposphere, but generally very little information is retrieved from the boundary layer (see example averaging kernels in Fig. 1 of Zhang et al. (2010)).

3.2. Regional and seasonal NAB estimates

Seasonal mean MDA8 NAB O_3 is consistently higher over the WUS than the EUS in both models (Fig. 1). During spring, AM3 simulates higher NAB over the high-altitude WUS than GEOS-Chem, which we attribute at least partially to a larger stratospheric influence in AM3 (Lin et al., 2012a) than in GEOS-Chem (Zhang et al., 2011). The diagnostics necessary to determine whether AM3 actually simulates more stratosphere-to-troposphere exchange of O_3 , or whether it mixes free tropospheric air (including the stratospheric component) into the planetary boundary layer more efficiently, were not archived from these simulations. However, an evaluation of AM3 O_3 profiles at sonde launch locations during the 2010 CalNex field campaign indicates that the model captures much of the observed vertical structure of O_3 throughout

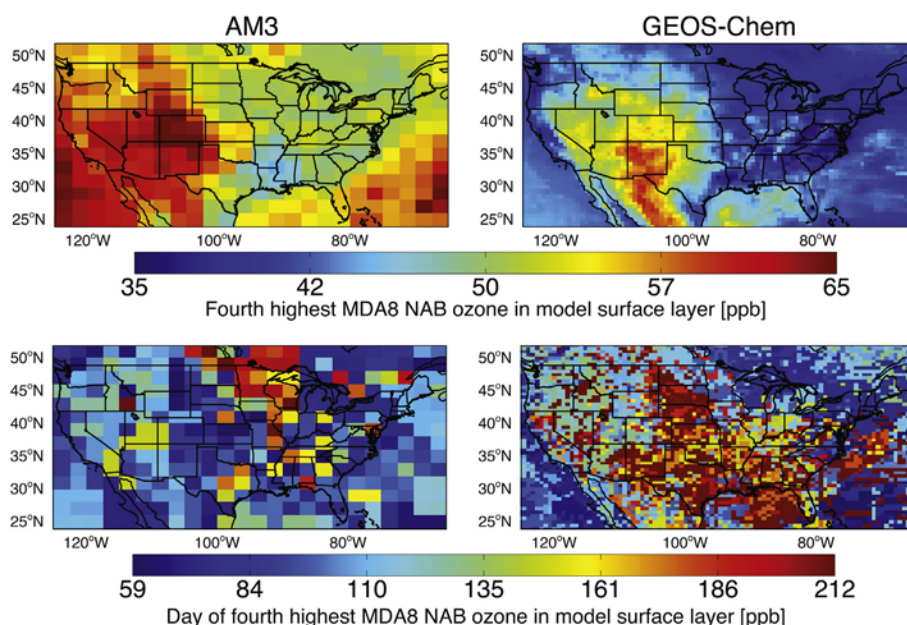


Fig. 2. Fourth highest MDA8 NAB O_3 between March 1 and August 31 2006 in the lowest model layer (top) and day of occurrence (bottom) for GFDL AM3 (left; $2^\circ \times 2^\circ$ horizontal resolution) and GEOS-Chem (right; $\frac{1}{2}^\circ \times \frac{2}{3}^\circ$) simulations.

the troposphere and lower stratosphere, including its day-to-day variability (Lin et al., 2012a, 2012b). During summer, the different simulated spatial patterns for NAB over the WUS are influenced by differences in the lightning NO_x sources (see Section 3.5).

Fig. 2 shows the spatial patterns of the fourth highest NAB value between March 1 and August 31. As the O_3 seasonal cycle is typically highest during the summer in polluted regions, we expect the fourth highest during this six-month period to represent reasonably this statistic over a full year. AM3 simulates the highest values over Colorado whereas GEOS-Chem indicates that the highest values occur over New Mexico (Fig. 2), reflecting excessive NAB associated with lightning NO_x and subsequent O_3 production and transport (Zhang et al., 2014). Due to different timing of these processes, AM3 simulates the fourth highest NAB values during spring over much of Colorado but GEOS-Chem simulates peak values over much of New Mexico during August (Fig. 2). Over Minnesota and Wisconsin, GEOS-Chem generally produces the fourth highest values in spring, but AM3 indicates that they occur in summer. Over the northeastern states and west coast, the fourth highest MDA8 concentrations generally occur during spring, though they occur later in the year over southeastern states, with occurrences generally later in GEOS-Chem than AM3.

The fourth highest values often occur during months when model biases are largest (Section 3.4), indicating that bias-correction techniques may be necessary for quantitatively accurate NAB estimates at specific locations and times. In the following sections, we analyze the model NAB estimates in the context of evaluating the total surface O_3 simulations with both space- and ground-based observations, a first step towards developing the process-level knowledge needed for accurate bias correction.

3.3. Constraints from space-based observations

With the exception of O_3 produced within the U.S. boundary layer from CH_4 or natural NMVOC and natural NO_x , NAB in surface air mixes downward from the free troposphere. We use 500 hPa products retrieved from both the OMI and TES instruments aboard the NASA Aura satellite to evaluate the potential for space-based

constraints on simulated mid-tropospheric total O_3 distributions. Our comparison thus evaluates the reservoir of mid-tropospheric O_3 , of any origin, that can mix into the planetary boundary layer. For context, the ratio of NAB to total O_3 over North America at 500 hPa in AM3 varies spatially and seasonally, with highest values generally in spring and a minimum contribution within any model grid cell of 70% (not shown).

During spring, AM3 estimates a stronger north-to-south O_3 gradient in the mid-troposphere than GEOS-Chem (compare first and third rows of Fig. 3). The satellite retrievals from both instruments suggest a stronger gradient than simulated with GEOS-Chem, which generally underestimates O_3 in the northern half of the United States compared both to TES (5–15 ppb) and OMI (up to 10 ppb). In contrast, AM3 mid-tropospheric O_3 is higher than the satellite products in the northern half of the domain, with a closer match to the OMI retrievals (generally within 5 ppb over the United States) than TES (positive biases up to 10–20 ppb). Prior direct evaluation of AM3 with O_3 sondes indicates biases of up to 10 ppb in AM3 at the high northern latitude measurement sites of Alert and Resolute at 500 and 800 hPa with little bias in spring at the mid-latitude North American sites of Edmonton, Trinidad Head, Boulder and Wallops Island (Naik et al., 2013), roughly consistent with the biases relative to OMI.

Both satellite instruments indicate a general decrease from spring into summer over the western and northern United States, but an increase over several southeastern states, northern Mexico, and the Gulf of Mexico (compare Figs. 3 and 4). The summertime spatial pattern of U.S. O_3 observed from space is broadly consistent with that estimated by interpolating upper tropospheric ozone-sonde measurements during August of 2006 (Cooper et al., 2007). While the increases from spring to summer in the mid-troposphere over the EUS may include a contribution from lofting of regional anthropogenic O_3 production, there is likely also a contribution from the larger lightning NO_x source in the free troposphere during summer. GEOS-Chem estimates a summertime mid-tropospheric O_3 enhancement at mid-latitudes, centered over the United States whereas AM3 simulates a gradient with O_3 generally increasing along the southwest-to-northeast direction (Fig. 4). Over Canada,

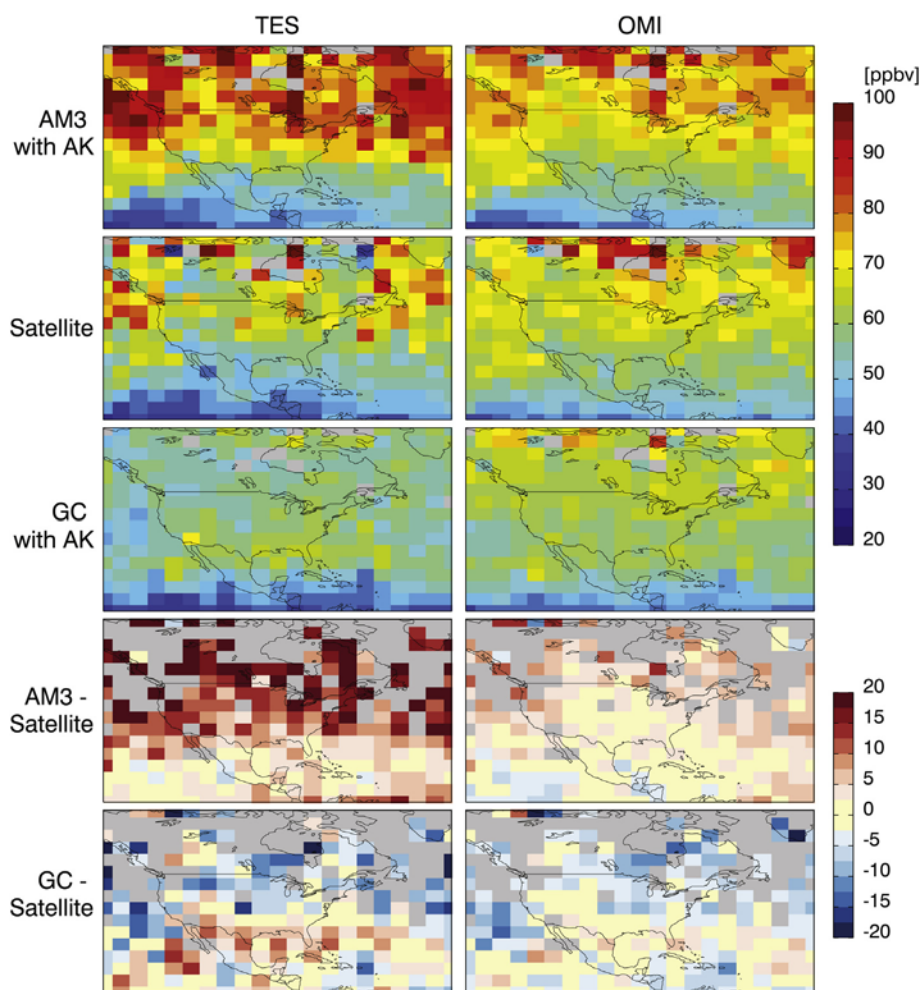


Fig. 3. Springtime (March–April–May average) mid-tropospheric O_3 as retrieved (second row) from the TES (left column) and OMI (right column) satellite instruments and as simulated with the GFDL AM3 (top row) and GEOS-Chem (third row) with the appropriate averaging kernels applied to daily average O_3 fields archived from the base model simulations. Gray boxes denote locations where no coincident TES and OMI data points meet the retrieval quality criteria. The simulations evaluated here are at coarse horizontal resolution ($\sim 2^\circ \times 2^\circ$) in both models. The 2005–2007 annual average bias of the satellite products (5.7 ppb for TES; 3.1 ppb for OMI) relative to ozone sondes between 20° and 60° N determined by Zhang et al. (2010) has been removed from the satellite products. The third and fourth rows show the difference of the simulated mid-tropospheric O_3 with each satellite product; gray boxes denote places where the OMI and TES retrievals disagree by over 10 ppb.

the AM3 model tends to be higher than both retrievals by up to 15–20 ppb during summer, as occurs during spring versus TES (but springtime biases are smaller compared to OMI).

We expect discrepancies between AM3 and observations during summer over forested boreal regions due to the use of a climatological wildfire inventory and the vertical distribution used to prescribe those emissions (Dentener et al., 2006), which lofts fire effluents into the mid-troposphere where they can efficiently produce O_3 and PAN (see also Section 3.5). GEOS-Chem includes fire emissions representative of the year 2006 and emits them only the planetary boundary layer. These model differences in wildfire treatment are likely reflected in the mid-tropospheric O_3 distributions shown in Figs. 3 and 4. They may also contribute to the different spatial distributions of simulated NAB at the surface, specifically the higher NAB estimated with AM3 over the northern United States and Canada relative to the NAB estimated with GEOS-Chem (Figs. 1 and 2).

In both Figs. 3 and 4, the models are generally more consistent with the OMI retrievals, which may reflect differences in the vertical sensitivity of the TES and OMI instruments. While the satellite retrievals provide useful qualitative constraints on the simulated mid-tropospheric distributions, the disagreement between OMI

and TES over many locations (gray boxes in Figs. 3 and 4) hinders their quantitative utility. The higher sampling frequency possible from instruments on geostationary satellites such as TEMPO (Hilsenrath and Chance, 2013) should improve the potential for space-based constraints on free-tropospheric and near-surface distributions.

We can nevertheless glean additional insights into the model vertical distributions of O_3 by examining differences in the models sampled with the two different averaging kernels (Figs. 3 and 4). For example, over Canada, GEOS-Chem indicates that OMI would measure higher O_3 than TES whereas AM3 indicates that TES should retrieve higher O_3 than OMI during both seasons. In the spring, the retrieved OMI product is generally higher than TES over this region. GEOS-Chem is generally within 10 ppb of the OMI product with a tendency to underestimate springtime mid-tropospheric O_3 over Canada, whereas AM3 is generally within 5 ppb of OMI over much of the United States and Canada, with a tendency towards a positive bias. During summer, TES is higher than OMI over Canada. The high O_3 bias over the EUS in AM3 is confined close to the surface (Fig. 5) since AM3 tends to underestimate free tropospheric O_3 , particularly over the convectively active Gulf of Mexico region where lightning NO_x is expected to be an important source of NAB O_3 . We conclude

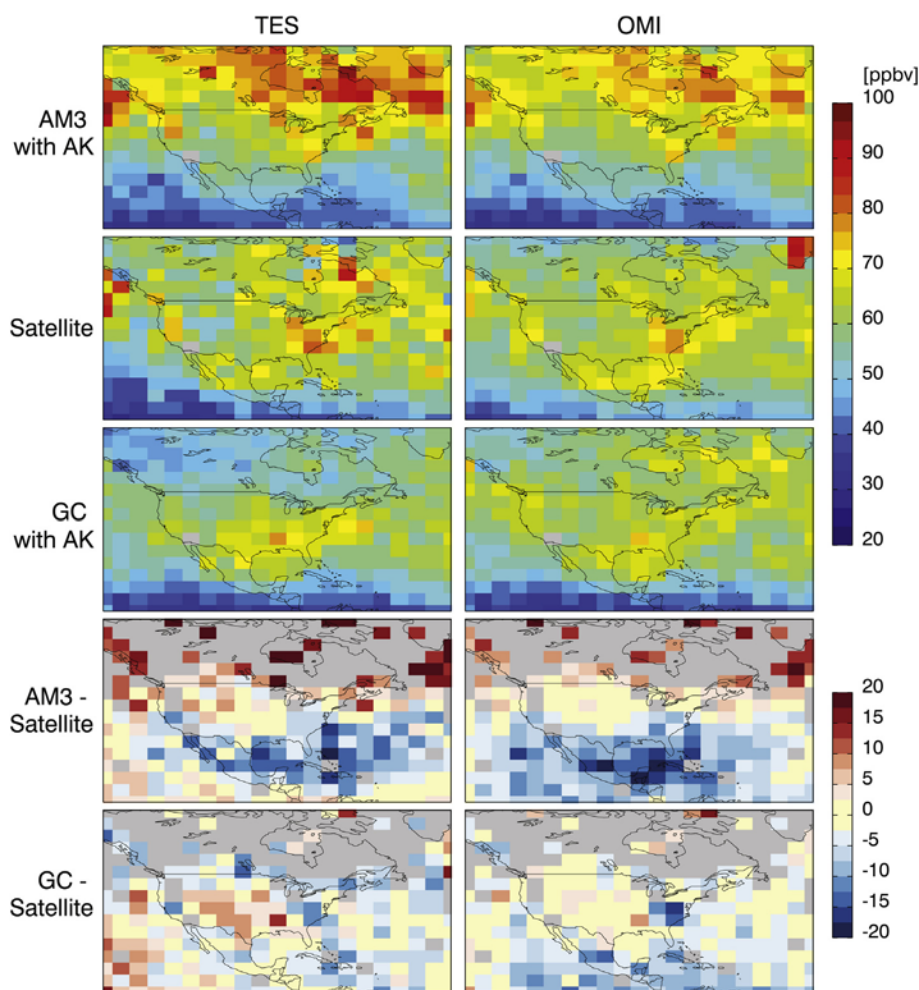


Fig. 4. As in Fig. 3 but for summer (June–July–August).

that the estimates from the models could bracket the true NAB in many cases, but caution that the ability of the models to bracket the satellite measurements does not necessarily imply accuracy in their NAB estimates.

3.4. Constraints from ground-based measurements

We use the CASTNet MDA8 O₃ observations to further constrain the model NAB estimates through an evaluation of the base simulations, which include all anthropogenic emissions, to simulate total surface O₃. Since NAB depends strongly on altitude (Fig. 1; references in Table 1), the remainder of our analysis separates the data by altitude to gain insight into the different processes shaping NAB distributions. Specifically, we divide the CASTNet sites into two groups: (1) below 1.5 km in elevation (low-altitude sites), primarily sites in the EUS, and (2) Intermountain West CASTNet sites with elevation greater than 1.5 km (high-altitude sites). This second category includes all high-altitude CASTNet sites except for those in California.

3.4.1. Seasonal variability

Fig. 5 shows the observed and simulated seasonal cycles at the CASTNet sites. At the high-altitude sites, both models are generally within 5 ppb of the regional mean observed values and usually fall within one standard deviation of the observed monthly mean values at the sites within the region. Consistent with the evaluation

in Section 3.3, the models tend to bracket the observations, but with notably different seasonal cycles. AM3 peaks in early spring, overestimating observed values in March but then declines to slightly underestimate observed values in June and July. In contrast, GEOS-Chem underestimates observed values from March through July but increases to overestimate observed values in August. The model differences are amplified in the NAB estimates: AM3 simulates a large seasonal decline in NAB from springtime (near 50 ppb) into summer (below 35 ppb) while GEOS-Chem estimates little seasonality in NAB (monthly mean values around 40 ppb).

At the low-altitude sites, AM3 exhibits a large positive bias in total surface O₃ in all months, most evident during summer. The exacerbation of the bias in summer at low-altitude sites implies a problem with O₃ produced from regional emissions, with isoprene–NO_x–O₃ chemistry a likely culprit given its different treatment in the models (Table 2; see Section 3.5). Both models show declining NAB levels from spring into summer, though the GEOS-Chem amplitude of the NAB seasonal cycle is smaller than that of AM3. The AM3 discrepancy with observations is much larger than the difference between the GEOS-Chem and AM3 NAB estimates except for March and April. If we assume that the model biases during March and April at both the high and low altitude sites are entirely due to NAB and correct the NAB estimates accordingly, the model NAB estimates would become more similar. While we conclude that the AM3 NAB at low-altitude sites is too high in March since we expect NAB to be lower than the observed value, it

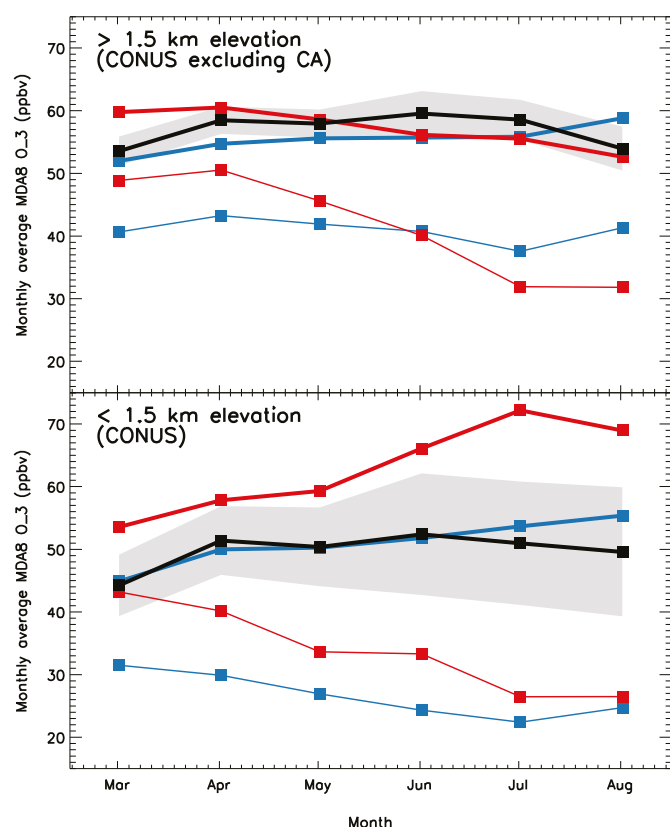


Fig. 5. Monthly mean MDA8 O₃ in surface air for March through August of 2006 in CASTNet observations (black) and the base simulations (thick lines) for the GEOS-Chem ($1/2^\circ \times 2/3^\circ$ horizontal resolution; blue) and GFDL AM3 ($\sim 2^\circ \times 2^\circ$ horizontal resolution red) simulations sampled at the CASTNet sites (using bilinear interpolation of the nearest four grid cells and sampling only on days with valid measurements) over the CONUS at altitudes a) above 1.5 km excluding California to focus on the InterMountain West region and b) below 1.5 km in altitude. Also shown are NAB estimates (thin lines) with GC (blue) and AM3 (red). The gray band delineates the one standard deviation range about the observed regional mean monthly values. (For interpretation of the references to color in this figure legend, the reader is referred to the web version of this article.)

is possible that NAB could actually be higher in an atmosphere with lower NO_x than under current conditions, due to more efficient O₃ production and slower chemical loss.

At the high-altitude sites in summer, the GEOS-Chem overestimate of observed O₃ has been attributed previously to an overestimate of O₃ associated with production from lightning NO_x plus subsequent transport when prescribing a higher production of NO_x from flashes at mid-latitudes and spatially scaling the source to match LIS-OTD climatological flash counts (Murray et al., 2012), which may lead to regional errors for a specific year (Zhang et al., 2014). The larger difference between the NAB estimates from the two models in August than between the simulated and observed total O₃ implies that the agreement with observations does not sufficiently constrain the NAB estimates.

3.4.2. Daily variability

Fig. 6 shows probability density distributions constructed from observed and simulated MDA8 O₃ in spring (top) and summer (bottom) sampled at the high-altitude (left) versus low-altitude (right) CASTNet sites, and statistics are summarized for the AM3 and high-resolution GEOS-Chem simulations in Table 3. We additionally include in Fig. 6 estimates from a coarse resolution version of the GEOS-Chem model (green) in order to

examine the extent to which differences in horizontal resolution contribute to the different NAB and total O₃ estimates in AM3 versus GEOS-Chem. In all cases, the NAB (dotted lines) differ more between the GEOS-Chem and AM3 models than between the high- versus low-resolution versions of GEOS-Chem. This conclusion also holds for the total O₃ distributions in spring. In summer, however, the total O₃ distributions in GEOS-Chem are more sensitive to the choice of horizontal resolution, presumably reflecting the larger contributions from local-to-regional photochemical production during this season and the importance of spatially resolving domestic anthropogenic and natural emissions distributions. Emery et al. (2012) found that the higher resolution CAMx model generally simulated higher WUS NAB than a coarse resolution version of GEOS-Chem, and better agreement has been noted between CAMx and the higher resolution version of GEOS-Chem (EPA, 2013). Simulation of higher WUS NAB by higher resolution models (Emery et al., 2012; Lin et al., 2012a) likely reflects improved resolution of topography and mesoscale meteorology at higher resolution and the damping of vertical eddy transport at coarser resolution (Wang et al., 2004; Zhang et al., 2011).

AM3 simulates a wider NAB range than GEOS-Chem (Fig. 6 and Table 3). This wider range of NAB may contribute to the wider total surface O₃ distribution in the AM3 versus GEOS-Chem standard simulations, which aligns more closely with the observed variability, except for O₃ simulated with the high-resolution GEOS-Chem model in summer at high-altitude sites. The relative skill of AM3 in capturing the variability of NAB despite its generally high bias implies that AM3 is useful for process-level analysis and for quantifying day-to-day variability.

In Table 3, we partition statistics for total and NAB O₃ in surface air into average versus high-O₃ days. We use observed values, rather than simulated values used in Zhang et al. (2011), to select for high-O₃ days in order to sample the same temporal subset from both models. Using the simulated total O₃ values would lead to subsets of different sizes given the individual model biases. During spring, the models robustly estimate NAB to be ~ 10 ppb higher on average at high-altitude than at low-altitude CASTNet sites, but AM3 estimates higher NAB levels than GEOS-Chem. During summer, the models also estimate higher NAB at high-altitude than at low-altitude sites, and average NAB levels decrease from spring to summer at low-elevation sites. GEOS-Chem suggests little change from spring to summer in average high-altitude NAB whereas AM3 simulates a decrease of over 10 ppb. At the high-altitude sites, both models suggest that NAB increases as total O₃ increases, although the sample size is small for events above 75 ppb and the average values for the different data subsets all fall within one standard deviation each other. At the low altitude sites, there is little change in the average NAB when selecting for observed values exceeding 60, 70, or 75 ppb. The variability in NAB, as measured by the standard deviation in Table 3, is similar in the two models at the low-elevation sites, but AM3 simulates more variability in NAB at the high-altitude sites than GEOS-Chem, particularly on high-O₃ days.

We next evaluate the ability of the models to capture observed day-to-day variability by correlating observed and simulated MDA8 O₃ in surface air at each CASTNet site, separately for the spring and summer seasons of 2006 (Fig. 7). During spring, the correlation coefficients between observations and total simulated surface O₃ over WUS sites are generally higher in GEOS-Chem, but the level of correlation in summer is maintained or improved in AM3 whereas it decreases in GEOS-Chem (Fig. 7). Over the EUS, the models show similar spatial patterns in their ability to reproduce the observed day-to-day variability. GEOS-Chem is generally better than AM3 over northern sites, whereas AM3 captures more of the variability over the southeastern sites in summer (Fig. 7).

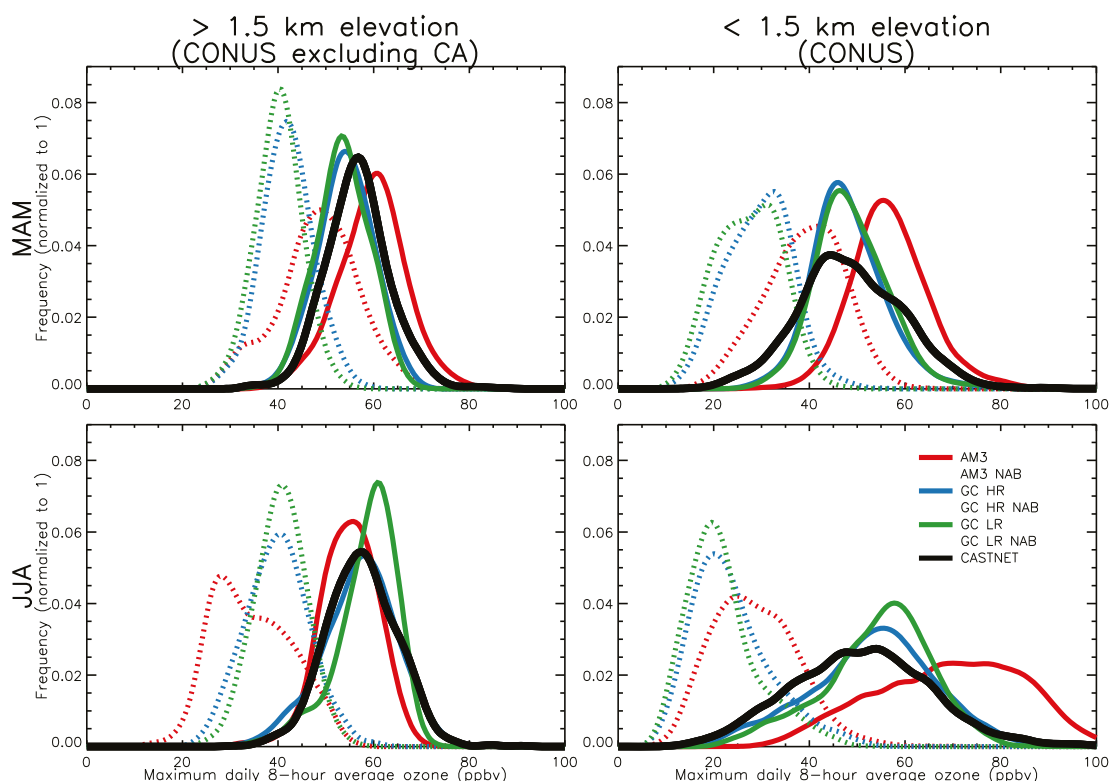


Fig. 6. Probability density curves calculated via kernel (Gaussian) density estimation with a bandwidth of 2 ppbv from surface MDA8 O_3 data over the CONTiguous United States (CONUS) during spring (top) and summer (bottom) and at high (left, excluding California sites) and low (right) elevation CASTNet sites: observed (black) and GFDL AM3 (red) and GEOS-Chem at low (green; $2^\circ \times 2.5^\circ$) and high (blue; $\frac{1}{2}^\circ \times \frac{1}{2}^\circ$) horizontal resolution (LR vs. HR) models sampled at the CASTNet sites for total (solid lines) and NAB (dashed lines) O_3 . (For interpretation of the references to color in this figure legend, the reader is referred to the web version of this article.)

Fig. 8 shows the correlation coefficients of the NAB estimates versus the simulated total O_3 , separately for spring and summer, for each model sampled at the CASTNet sites that were used in Fig. 7 to evaluate the simulated daily variability. Over the Intermountain WUS sites, the models robustly indicate that variability in NAB drives a substantial portion of the total surface O_3 variability in both seasons, but with a stronger influence (higher correlations) during spring. AM3 generally indicates a stronger role for NAB in contributing to variability in total surface O_3 at the sites in Florida

Table 3

Summary statistics of seasonal mean MDA8 total and NAB O_3 in surface air (ppb) as observed and estimated with the GFDL AM3 and GEOS-Chem (GC) models, segregated by altitude, season, and observed values. California is excluded to focus on the Intermountain West.

Season	Filter	N	OBS	AM3 base	GC base	AM3 NAB	GC NAB
Above 1.5 km (excluding CA)							
MAM	None	993	57 ± 7	60 ± 7	54 ± 6	48 ± 8	42 ± 5
MAM	Obs ≥ 60	300	64 ± 4	63 ± 7	58 ± 6	52 ± 8	45 ± 5
MAM	Obs ≥ 70	33	73 ± 4	66 ± 6	62 ± 4	55 ± 7	47 ± 5
MAM	Obs ≥ 75	7	80 ± 4	65 ± 7	61 ± 2	56 ± 8	50 ± 3
JJA	None	899	58 ± 7	55 ± 6	57 ± 8	35 ± 8	40 ± 7
JJA	Obs ≥ 60	344	65 ± 4	58 ± 5	59 ± 7	38 ± 8	41 ± 6
JJA	Obs ≥ 70	38	73 ± 5	61 ± 4	62 ± 7	43 ± 8	42 ± 6
JJA	Obs ≥ 75	9	80 ± 6	64 ± 4	64 ± 6	47 ± 6	42 ± 3
Below 1.5 km							
MAM	None	5769	49 ± 11	57 ± 8	48 ± 8	39 ± 8	29 ± 7
MAM	Obs ≥ 60	969	65 ± 6	64 ± 8	57 ± 8	37 ± 8	29 ± 7
MAM	Obs ≥ 70	175	75 ± 6	69 ± 8	63 ± 10	36 ± 10	31 ± 8
MAM	Obs ≥ 75	58	82 ± 6	71 ± 10	68 ± 12	36 ± 11	34 ± 9
JJA	None	5583	51 ± 15	69 ± 15	54 ± 14	29 ± 9	24 ± 8
JJA	Obs ≥ 60	1509	69 ± 9	76 ± 13	63 ± 11	30 ± 9	25 ± 9
JJA	Obs ≥ 70	537	78 ± 8	77 ± 13	67 ± 12	30 ± 9	27 ± 10
JJA	Obs ≥ 75	294	83 ± 8	76 ± 14	69 ± 14	31 ± 9	28 ± 10

and Texas. Over the central states and over the inland mid-Atlantic region, the NAB is more strongly correlated with total surface O_3 in GEOS-Chem than in AM3; the stronger correlation in GEOS-Chem in these regions may arise from soil NO_x emissions, which respond to meteorological variability in GEOS-Chem whereas AM3 uses a monthly climatology. At the EUS sites in Fig. 8, the NAB in both models is poorly correlated, and in some cases, anti-correlated with the total simulated surface O_3 . The highest total surface O_3 events over the EUS are thus generally decoupled from the highest NAB events, consistent with the current understanding that regional pollution is the dominant influence on total O_3 distributions in this region.

We select four sites, encircled in black in Figs. 7 and 8, to probe more deeply the day-to-day variability in NAB and total surface O_3 . The time series at these sites (Fig. 9a and b) provide evidence at the local scale for our assessment of regional and seasonal biases. At the two western U. S. sites (Gothic, CO and Grand Canyon NP, AZ) in Fig. 9a, the 6-month average NAB is nearly the same in both models, but this reflects little seasonal variation in the GC NAB (thin blue line) versus a sharp seasonal decline from spring into summer in AM3 (thin red line). The standard deviation is twice as large in AM3 as in GEOS-Chem, consistent with the frequency distributions of NAB in Fig. 6 (left side); AM3 also captures the observed variability. Despite the summertime high bias in AM3 at the two EUS sites (M.K. Goddard, PA and Georgia Station, GA), AM3 correlates at least as well with the observations as GEOS-Chem (Figs. 7 and 9).

3.5. Processes contributing to inter-model differences in total and NAB surface O_3

We use the sites in Fig. 9a to examine the role of specific processes in contributing to differences in the GEOS-Chem and AM3

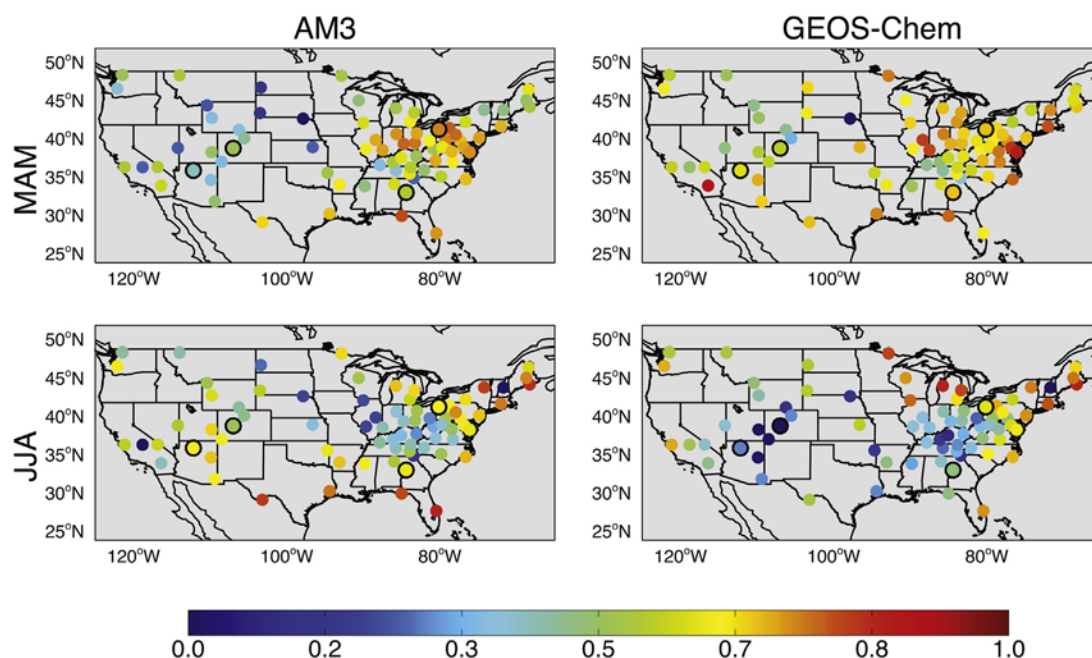


Fig. 7. Correlation coefficients (r) of observed MDA8 O_3 in surface air with that simulated by the GFDL AM3 (left) and GEOS-Chem (right) models during spring (MAM; top row) and summer (JJA; bottom row). Black circles mark the sites used in Fig. 9 and discussed in Section 3.5.

Base and NAB simulations. Superimposed in Fig. 9a and b are results from a separate simulation (Lin et al., 2014) in which a stratospheric O_3 tracer (O3Se90) was available (orange line), tagged relative to the e90 tropopause (Prather et al., 2011) as described in Lin et al. (2012a). The high summertime correlation of O3Se90 and NAB at the WUS sites (Fig. 9a) does not imply that stratospheric O_3 intrusions are the dominant factor. The magnitude of the O3Se90 enhancements in summer do not account for all of the episodic NAB enhancements. Rather, this result implies that other sources

enhance NAB free tropospheric O_3 , which then mixes into the surface air alongside the O3Se90 tracer in the model. We interpret the high correlations in both seasons at the EUS sites (r^2 ranges from 0.72 to 0.86) in a similar manner: the O3Se90 indicates a larger influence of O_3 mixing down from the free troposphere.

3.5.1. Deep stratospheric intrusions over the WUS in spring

As described by Lin et al. (2012a), stratospheric O_3 drives a substantial portion of the daily variability in observed springtime

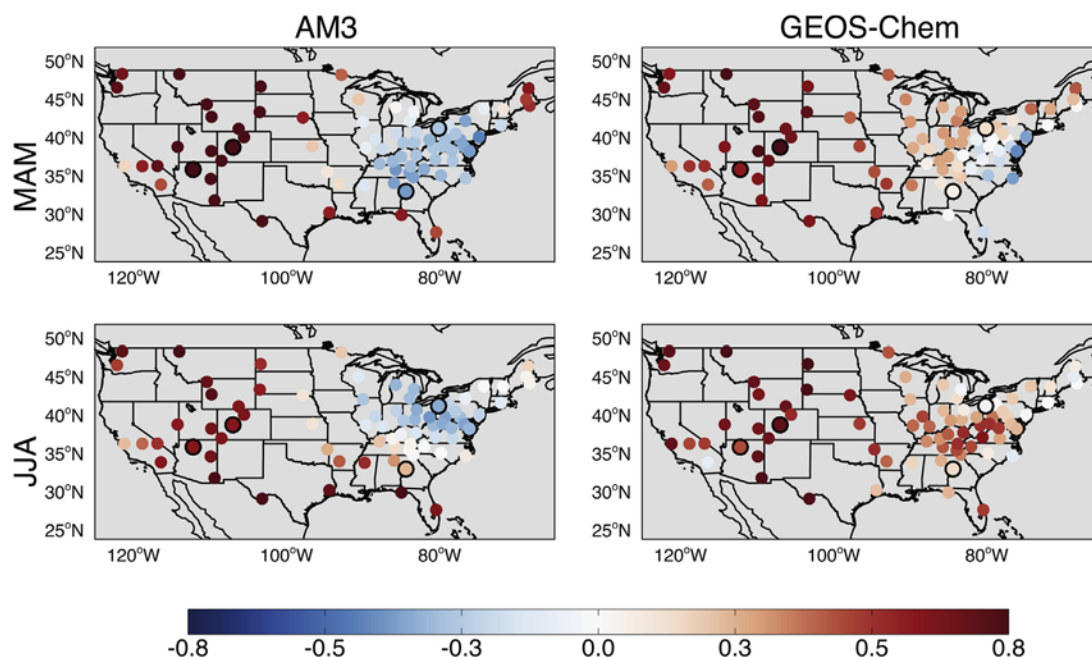
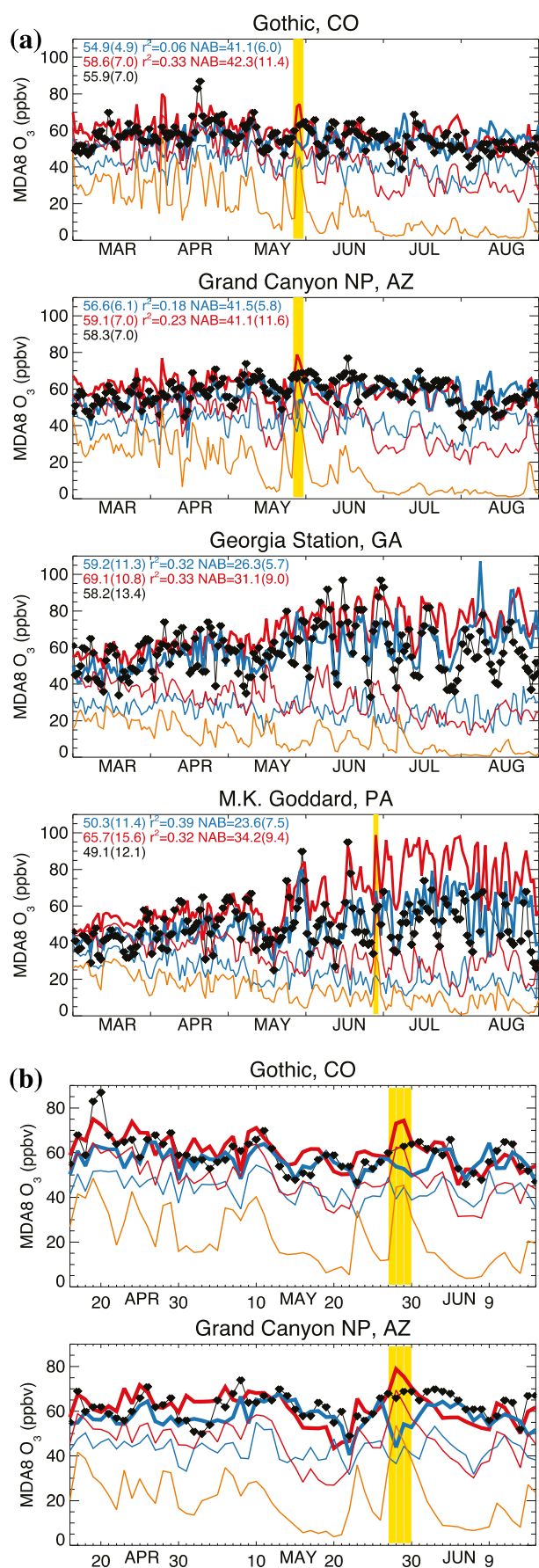


Fig. 8. As in Fig. 7 but for simulated NAB versus simulated total O_3 in surface air. The color bar saturates to emphasize regional patterns. (For interpretation of the references to color in this figure legend, the reader is referred to the web version of this article.)



O₃ over the WUS. Inspection of Fig. 9a (top two panels) shows that the episodic enhancements in the O3Se90 tracer can explain much of the episodic enhancements in NAB. A caveat is that the magnitude of the stratospheric contribution is an upper limit due to the definition of the O3Se90 tracer, which could be tagging O₃ in the lower stratosphere that originated in the troposphere (see discussions in Lin et al. (2012b) and Zhang et al. (2014)). Nevertheless, the strong correlation of the orange and red lines in Fig. 9a implies a key role for mixing of free tropospheric air into the planetary boundary layer in driving day-to-day variability in NAB O₃ levels.

For illustrative purposes, we focus on an event during late May of 2006 at the Gothic and Grand Canyon sites, during which the AM3 model NAB (thin red line in Fig. 9a and b) spikes, with an associated increase in the simulated total O₃ (thick red line). In contrast, GEOS-Chem NAB (thin blue line) decreases, as does total O₃ (thick blue line) during this event. The opposing trends in the models during this event raise questions as to whether both models simulate a mixing event but import different NAB levels, or whether the boundary layer in AM3 mixes more vigorously with the free troposphere than in GEOS-Chem. The observations (black) increase during this period, as in AM3, but the model overestimates the observed values on May 28 and 29. The O3Se90 tracer (orange line in Fig. 9a and b) suggests that the AM3 model is simulating surface O₃ enhancements associated with a stratospheric intrusion; the spatial pattern of these enhancements aligns with the observed spatial pattern of enhanced ground-level O₃ at the CASTNet sites (not shown). Fig. 9a further suggests that these events drive much of the variability in NAB at high-altitude western sites in spring, consistent with earlier findings for April through June of 2010 (Lin et al., 2012a).

3.5.2. Wildfires over the EUS in spring and summer

There are several EUS events during spring and summer where AM3 simulates a localized spike in NAB that is not simulated by GEOS-Chem, which we attribute to at least partially to the different treatment of wildfire emissions in the models (Table 2). For example, there is an extreme “NAB event” in the AM3 model on June 28, 2006 at the Pennsylvania CASTNet site in Fig. 9a. AM3 estimates NAB values above 60 ppb, exceeding the total observed value of about 60 ppb, while GEOS-Chem simulates NAB below 20 ppb (Fig. 9a, yellow highlight). We find that the use of a year-specific fire inventory (as is done in the GEOS-Chem simulations) versus a climatology leads to differences of 10 ppb for the June 28, 2006 event in AM3 (not shown). In AM3, the recommendations from Dentener et al. (2006) are applied to vertically distribute

Fig. 9. a. MDA8 O₃ in surface air observed (black) at four CASTNet sites for March through August 2006 (highlighted by black circles in Figs. 7 and 8), and simulated with the GEOS-Chem (blue thick lines) and GFDL AM3 (red thick lines) models. Also shown are NAB estimates with GEOS-Chem (blue thin lines) and GFDL AM3 (red thin lines) and an estimate of stratospheric O₃ influence in the AM3 model (orange lines) following the method described in Lin et al. (2012b) from a simulation described in Lin et al. (2014). Statistics in the upper left corner of each panel are for the entire March through August period: the mean and standard deviation (in parentheses) of total surface O₃ as observed (black) and simulated with GEOS-Chem (blue) and GFDL AM3 (red); coefficients of determination for each model versus the observations (see also correlation coefficients in Figs. 7 and 8 for separate correlations during spring and summer); the mean and standard deviation of the MDA8 NAB O₃ simulated with each model. The stratospheric O₃ tracer (orange), which can be interpreted more broadly as a diagnostic of mixing between the free troposphere and the surface, correlates strongly at all sites (r^2 ranges from 0.72 to 0.86) with the NAB (red). Yellow highlighted days at the western U.S. sites and PA site are discussed in Section 3.5.1. The Gothic, CO panel is adapted from Figs. 3–75 of the U.S. EPA Integrated Science Assessment for O₃ (EPA, 2013). **b.** As in Fig. 9a but for mid-April through mid-June at the two high-altitude Western U.S. sites in order to focus in on the stratospheric intrusion event discussed in Section 3.5. (For interpretation of the references to color in this figure legend, the reader is referred to the web version of this article.)

biomass burning emissions north of 25°N, placing 40% of the total emissions between 3 and 6 km (see their Table 4) over boreal North America. This lofting of fire effluents likely contributes to the summertime O₃ overestimates at 500 hPa over Canada (Fig. 4). Vertical mixing of NAB O₃ from the free troposphere into surface air in the AM3 model is indicated by associated enhancements of the O3Se90 tracer on days with high NAB. In contrast, biomass burning is emitted only in the boundary layer in GEOS-Chem, likely resulting in less efficient O₃ production and subsequent long-range transport. The GEOS-Chem approach appears more consistent with the observations.

3.5.3. Lightning NO_x over the southwestern United States in summer

During August at the two WUS sites in Fig. 9a, the models reverse their relative rankings of simulated NAB relative to springtime, with the GEOS-Chem NAB as much as 10–20 ppb higher than AM3 NAB. In notable contrast to the spring, GEOS-Chem overestimates the observed O₃ values. We attribute the summertime overestimate and poor correlations of GEOS-Chem with the observed values over WUS sites in Figs. 7 and 9a to the lightning NO_x source and subsequent transport. GEOS-Chem produces approximately 10 times more lightning NO_x than AM3 over the southwestern states during summer (0.018 Tg N in AM3 versus 0.159 Tg N in GC within the region 26°N–42°N, 124°W–97°W) and the models further differ in their spatial distributions of the lightning NO_x source (Table 2). This source has been reduced in a newer version of GEOS-Chem, decreasing simulated NAB O₃ over these regions (Zhang et al., 2014).

3.5.4. Isoprene oxidation chemistry over the EUS in summer

Earlier work (e.g. Fiore et al., 2002, 2003) demonstrated that NAB is fundamentally different between the EUS and the WUS, with the EUS more strongly controlled by regional photochemistry, where the O₃ lifetime in the planetary boundary layer is as short as 1–2 days and isoprene–NO_x–O₃ chemistry dominates much of the region from May through September (Jacob et al., 1995). At the two EUS sites in Fig. 9a (M.K. Goddard, PA and Georgia Station, GA), we attribute some of the differences in the summertime simulations to the isoprene oxidation mechanism (Table 2) that would tend to reduce O₃ production in GEOS-Chem relative to AM3 due to isoprene ozonolysis serving as a more important loss pathway for NAB in GEOS-Chem (Fiore et al., 2002; Mickley et al., 2001). These differences in isoprene oxidation chemistry could at least partially explain the higher NAB in AM3 during the isoprene emission season (i.e., a longer O₃ lifetime in the AM3 boundary layer). The largest inter-model differences in NAB, however, occur in spring when transported sources are more important than regional production involving natural sources.

The isoprene oxidation chemistry likely also contributes to the large bias in AM3 total surface O₃. GEOS-Chem assumes a much higher yield of isoprene nitrates from the reaction of isoprene hydroxyperoxy radicals with NO and assumes that they are a permanent sink for NO_x (Table 2). In contrast, AM3 assumes an 8% isoprene nitrate yield and allows 40% of the products to recycle back to NO_x on the basis of observational constraints from field campaigns (Horowitz et al., 2007; Perring et al., 2009). Earlier work with predecessors of the models used here suggests that these differences may explain over 10 ppb of the high bias in AM3 relative to GEOS-Chem over the EUS in summer (Fiore et al., 2005). The fact that GEOS-Chem best captures the observations implies that the additional O₃ production from isoprene oxidation using the field-based constraints on isoprene nitrates must be offset by larger O₃ losses, such as may occur through additional HO_x uptake by aerosol

(Mao et al., 2013) and halogen-induced O₃ destruction (Parrella et al., 2012).

4. Inter-annual variability in NAB MDA8 O₃ estimates in surface air

The 27-year AM3 NAB simulation (1981–2007) enables us to define spring and summer climatologies of seasonal mean NAB O₃ in surface air, and to quantify the year-to-year variability as the standard deviation of the annual seasonal mean values (Fig. 10). The seasonal mean spatial patterns are similar to those in 2006 (Fig. 1), with little year-to-year variation over much of the country. Fig. 10 also includes the climatological fourth highest MDA8 value between March 1 and August 31 over the multi-decadal simulation. We emphasize that these estimates are subject to the biases diagnosed above in comparison to observations. In particular, NAB estimates over the EUS are probably too high in AM3. The variability over central Texas and central Mexico in the fourth highest values may indicate year-to-year variations in events involving NAB production from lightning NO_x and convective mixing. Large variability in both mean NAB levels and the highest events is simulated over Western Colorado in spring, with standard deviations of 2–3 ppb, likely reflecting variability in year-to-year influence from stratospheric O₃ intrusions.

Jaffe (2011) noted regionally coherent year-to-year variability in the number of high-O₃ events at high-altitude western U.S. measurement sites in both spring and summer and we examine here the potential contribution of NAB to this observed variability. Specifically, Jaffe (2011; see their Fig. 6) found that the number of O₃ events above levels of 65, 70, and 75 ppb varied together, with the lowest and highest number of springtime events occurring in 1997 and 1999, respectively; for summer, the lowest and highest years were 1997 and 2002. We follow the approach of Wang et al. (2009; see their Fig. 5) to illustrate simultaneously the model skill at capturing the observed values, and the simulated NAB contribution to observed levels within specific ranges for total surface O₃. Fig. 11 shows the AM3 NAB contributions throughout the overall observed distributions for 2006 in comparison to a low versus high year for observed high-O₃ events at the 11 high-altitude WUS sites in Figs. 5 and 6. Note that the highest years in Fig. 11 differ for spring and summer, but the lowest year is 1997 in both seasons.

For observed O₃ events above 60 ppb, AM3 tends to overestimate observations during spring but does not exhibit any systematic bias during summer. Furthermore, the model captures events up to 80 ppb during spring of 1999, though in other years there is a general tendency to underestimate events above 75 ppb. This finding is in contrast to those from higher-resolution models including the GEOS-Chem version used here, which underestimates events above 60 ppb (Zhang et al., 2011). During all years and both seasons shown in Fig. 11, there is a tendency for the median simulated NAB contribution to increase from observed values of 40 ppb to those in the 70 ppb range, with 75th percentile values reaching 50–60 ppb for observed values above 60 ppb during 2006 and 1999, implying that enhanced NAB levels contribute to the higher observed values. This interpretation is consistent with the findings of Lin et al. (2012a) that stratospheric O₃ intrusions over the high-altitude WUS drive much of the observed day-to-day variability in spring, as well as with Jaffe (2011) who suggests that a large-scale process drives coherent variability at the monitoring sites in this region.

Consistent with earlier work (Fiore et al., 2003), Fig. 11 shows that summertime NAB levels are typically much lower than in spring, with maximum values nearly always below 60 ppb and 75th percentile values generally below 50 ppb. Jaffe (2011) suggested

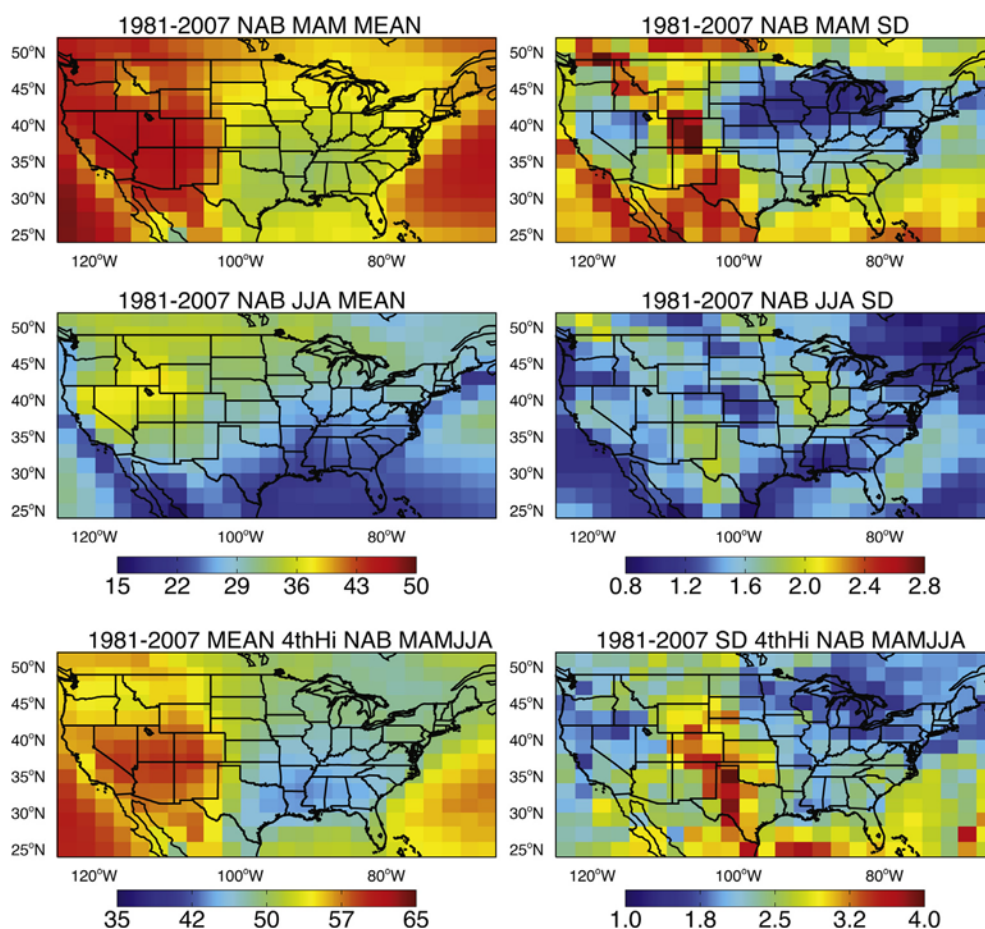


Fig. 10. Climatological (1981–2007) average (left) and standard deviation (right) of spring (top) and summer (middle) seasonal mean MDA8 NAB O_3 , and of the fourth highest value between March 1 and August 31 (bottom) as estimated with the GFDL AM3 model simulation in which North American anthropogenic emissions are set to zero.

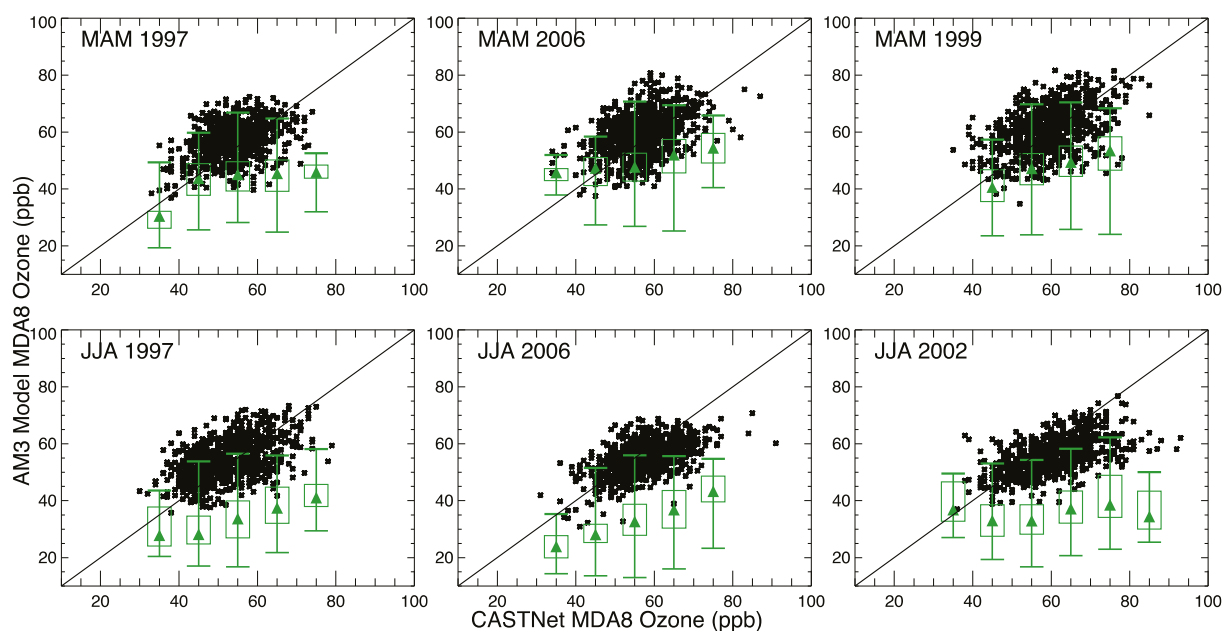


Fig. 11. GFDL AM3 simulated daily maximum 8-h (MDA8) surface O_3 versus observed values (black) and AM3 NAB statistics (green) at 11 Intermountain Western U.S. CASTNet sites above 1.5 km altitude for a “low- O_3 ” year (left column) and “high- O_3 ” year (right column) to provide context for the year 2006 (middle column) during spring (top panel) and summer (bottom panel), following the approach of Wang et al. (2009; see their Fig. 5). The 1:1 line (solid black) and a 60 ppb threshold (dashed line) are shown. Box and whisker plots show the median (triangle), 25th–75th range (box) and minimum and maximum NAB values (vertical lines) for 10 ppb bins of observed O_3 values. The “low” and “high” years are selected from Fig. 6 of Jaffe (2011). (For interpretation of the references to color in this figure legend, the reader is referred to the web version of this article.)

that summertime inter-annual variability is strongly influenced by wildfire activity. The lack of year-to-year variations in wildfires in this version of the AM3 model may contribute to its underestimate of the highest events in 2002 and 2006, which were the first and second highest fire activity years for the 1997–2006 period analyzed by Jaffe (2011).

5. Conclusions and recommendations

On the basis of health evidence, the level of the National Ambient Air Quality Standard (NAAQS) for ground-level O₃ has been lowered in recent years, pushing closer to “background” levels. In the past, the U.S. Environmental Protection Agency considered model-based estimates of background O₃ as part of the process for setting the NAAQS. These model-based estimates, previously called “Policy-Relevant Background”, are now termed “North American Background” (NAB), which is defined to be background levels that would exist in the absence of North American anthropogenic emissions. Identifying high-background events is crucial for determining whether an observation merits consideration for “exceptional event” status, which exempts a particular observation from counting towards non-attainment if it can be shown that the event occurred due to processes beyond the control of U.S. air quality management options. The model simulations presented here can provide information on the frequency of such events and the individual components contributing to NAB, including O₃ originating from international pollution, wildfires, or the stratosphere.

As a first step towards assessing our understanding of NAB and its components, we briefly reviewed recent model estimates (Table 1). We then evaluated total surface O₃ and NAB estimates from two independent models (GEOS-Chem and AM3) for March through August of 2006, using comparisons between the base simulations and space-based and ground-based measurements to place constraints on the model estimates. A 27-year NAB simulation in the AM3 model provides context for our two-model analysis and indicates that 2006 is a typical year in terms of its spatial and seasonal patterns in NAB, though 2006 NAB levels are generally higher than the climatological averages (compare Fig. 10 with 1 and 2). The largest variability in mean NAB MDA8 estimated with AM3 occurs over Idaho, western Colorado and Wyoming, and New Mexico, with standard deviations of over 2 ppb; the largest variability in the fourth highest MDA8 NAB occurs over Colorado and Texas (Fig. 10). A comparison of low- versus high-O₃ years at high-altitude western U.S. (WUS) sites indicates a role for NAB in driving year-to-year differences in the frequency of springtime high-O₃ events (Fig. 11).

At high-altitude WUS sites, the GEOS-Chem and AM3 models consistently show higher NAB than at low-altitude sites, but the magnitude and day-to-day variability often differs (Figs. 1, 5, 6 and 9a, Table 3). In some months (e.g., August), the larger differences between the NAB estimates from the two models than between the simulated and observed total O₃, imply that agreement with observations does not sufficiently constrain the NAB estimates. While AM3 indicates a seasonal decline of NAB into summer over this region, GEOS-Chem suggests a relatively weak seasonal cycle associated with an increase of influence from lightning NO_x in that model during the late summer (Figs. 5 and 9). Higher stratosphere–troposphere exchange in AM3 may explain the springtime NAB enhancement in the free troposphere relative to GEOS-Chem (Fig. 3), which, followed by more vigorous mixing between the free troposphere and boundary layer, may explain the higher NAB in surface air during this season in AM3 (Fig. 1).

At low-altitude sites, such as over the EUS, the models consistently show lower NAB levels than at high-altitude sites, as in

earlier work (Table 1). We find that the highest total surface O₃ events over the EUS are often decoupled from the highest NAB events (Fig. 8), consistent with the understanding that regional pollution is the dominant influence on total O₃ distributions there. Over the EUS, uncertainties in isoprene–NO_x–O₃ chemistry (Table 2) likely contribute to differences in simulated total O₃, and to a lesser extent, NAB estimates.

We find little evidence that horizontal resolution is a major contributor to differences in mean NAB estimates in the models (Fig. 6), consistent with EPA (2013). Higher resolution refines spatially local NAB estimates, including at the tails of the distribution. It also resolves better the impact from local and regional emissions, as evidenced by the larger differences associated with resolution in summertime distributions when photochemical production peaks over many U.S. regions (Fig. 6). We conclude that simulated NAB distributions reflect large-scale synoptic transport that is resolved sufficiently at the relatively coarse scale of global models, with the NAB differences mainly stemming from different treatments of NAB sources such as stratospheric O₃, boreal fires, and lightning NO_x. The regional and seasonal variability in these driving processes further manifests as differences in the model timings of the fourth highest NAB over many regions (Fig. 2).

Future efforts to determine the processes contributing to model differences, and to the biases in individual models versus observations, would benefit from evaluation with daily O₃ vertical profiles as measured by sondes, consistently defined tracers of stratospheric influence (e.g., the O3Se90 tracer in AM3), as well as daily three-dimensional archival of other chemical species (e.g., CO, PAN, H₂O) that can aid in disentangling tropospheric versus stratospheric origins and from meteorological variables (e.g., mixing depth, mass fluxes) to diagnose the role of mixing processes. The routine use of synthetic tracers could further aid in distinguishing between model differences in transport, dilution, and mixing versus chemical evolution during transport. Improved estimates of NAB in a given region and season will require better constraints on, for example: lightning NO_x for central and southwestern states in summer; transported stratospheric O₃ over the high-altitude WUS in spring; isoprene chemistry and its impact on chemical processing and NAB lifetime over the EUS in summer; and wildfires, which may influence NAB throughout the nation from late spring into summer.

We propose that future multi-model studies target limited time periods to enable process-oriented analysis during field campaigns when ground-based and satellite observations are supplemented with a broader suite of observations from intensive aircraft flights and balloon launches. If combined with a thorough evaluation of O₃ precursors, such analysis should hasten progress towards understanding the impact of specific sources on NAB O₃. We further recommend developing bias-correction techniques, such as those routinely applied in numerical weather prediction, to improve the accuracy of local NAB estimates. As a first step, simple assumptions assuming the bias is entirely driven by one process (e.g., as applied to the stratospheric O₃ estimates from the AM3 model by Lin et al. (2012a)) can be applied to individual models and then used to generate a multi-model estimate with uncertainties. The two models analyzed here often bracket the observations (Figs. 3–6 and 9), thereby indicating different sources of error, which leads us to conclude that a multi-model approach can harness unique capabilities of different modeling systems and thus provide more accurate NAB estimates than a single model.

Acknowledgments

We acknowledge support from the NASA Air Quality Applied Sciences Team (NNX12AF15G to AMF; NNX11AH93G to DJJ), and

the NOAA Ernest F. Hollings Scholarship program (JTO). We are grateful to P. Dolwick (U.S. EPA) for useful discussions and comments, and suggestions from anonymous review. The information in this article has been subjected to review by the National Center for Environmental Assessment, U.S. Environmental Protection Agency, and approved for publication. The views expressed in this manuscript are those of the authors and do not necessarily represent the views or policies of the U.S. Environmental Protection Agency.

References

- Baumgardner, R.E., Lavery, T.F., Rogers, C.M., Isil, S.S., 2002. Estimates of the atmospheric deposition of sulfur and nitrogen species: clean air status and trends network, 1990–2000. *Environ. Sci. Technol.* 36, 2614–2629.
- Beer, R., 2006. TES on the aura mission: scientific objectives, measurements, and analysis overview. *Geosci. Remote Sens. IEEE Trans.* 44, 1102–1105.
- Bey, I., Jacob, D.J., Yantosca, R.M., Logan, J.A., Field, B.D., Fiore, A.M., Li, Q., Liu, H.Y., Mickley, L.J., Schultz, M.G., 2001. Global modeling of tropospheric chemistry with assimilated meteorology: model description and evaluation. *J. Geophys. Res.* 106, 23073–23095.
- Brown-Steiner, B., Hess, P., 2011. Asian influence on surface ozone in the United States: a comparison of chemistry, seasonality, and transport mechanisms. *J. Geophys. Res.* 116, D17309.
- Collins, W.J., Derwent, R.G., Garnier, B., Johnson, C.E., Sanderson, M.G., Stevenson, D.S., 2003. Effect of stratosphere-troposphere exchange on the future tropospheric ozone trend. *J. Geophys. Res. Atmos.* 108, 8528.
- Cooper, O.R., Trainer, M., Thompson, A.M., Oltmans, S.J., Tarasick, D.W., Witte, J.C., Stohl, A., Eckhardt, S., Lelieveld, J., Newchurch, M.J., Johnson, B.J., Portmann, R.W., Kalnajs, L., Dubey, M.K., Leblanc, T., McDermid, I.S., Forbes, G., Wolfe, D., Carey-Smith, T., Morris, G.A., Lefer, B., Rappenglück, B., Joseph, E., Schmidlin, F., Meagher, J., Fehsenfeld, F.C., Keating, T.J., Van Curen, R.A., Minschwaner, K., 2007. Evidence for a recurring eastern North America upper tropospheric ozone maximum during summer. *J. Geophys. Res. Atmos.* 112, D23304.
- Dentener, F., Kinne, S., Bond, T., Boucher, O., Cofala, J., Generoso, S., Ginoux, P., Gong, S., Hoelzemann, J.J., Ito, A., Marelli, L., Penner, J.E., Putaud, J.P., Textor, C., Schulz, M., van der Werf, G.R., Wilson, J., 2006. Emissions of primary aerosol and precursor gases in the years 2000 and 1750 prescribed data-sets for AeroCom. *Atmos. Chem. Phys.* 6, 4321–4344.
- Donner, L.J., Wyman, B.L., Hemler, R.S., Horowitz, L.W., Ming, Y., Zhao, M., Golaz, J.-C., Ginoux, P., Lin, S.J., Schwarzkopf, M.D., Austin, J., Alaka, G., Cooke, W.F., Delworth, T.L., Freidenreich, S.M., Gordon, C.T., Griffies, S.M., Held, I.M., Hurlin, W.J., Klein, S.A., Knutson, T.R., Langenhorst, A.R., Lee, H.-C., Lin, Y., Magi, B.L., Malyshev, S.L., Milly, P.C.D., Naik, V., Nath, M.J., Pincus, R., Ploshay, J.J., Ramaswamy, V., Seman, C.J., Shevliakova, E., Sirutis, J.J., Stern, W.F., Stouffer, R.J., Winton, M., Wittenberg, A.T., Zeng, F., 2011. The dynamical core, physical parameterizations, and basic simulation characteristics of the atmospheric component AM3 of the GFDL global coupled model CM3. *J. Clim.* 24, 3484–3519.
- Emery, C., Jung, J., Downey, N., Johnson, J., Jimenez, M., Yarwood, G., Morris, R., 2012. Regional and global modeling estimates of policy relevant background ozone over the United States. *Atmos. Environ.* 47, 206–217.
- Emmons, L.K., Walters, S., Hess, P.G., Lamarque, J.F., Pfister, G.G., Fillmore, D., Granier, C., Guenther, A., Kinnison, D., Laepple, T., Orlando, J., Tie, X., Tyndall, G., Wiedinmyer, C., Baughcum, S.L., Kloster, S., 2010. Description and evaluation of the model for ozone and related chemical tracers, version 4 (MOZART-4). *Geosci. Model Dev.* 3, 43–67.
- Environmental Protection Agency (EPA), 2006. In: Agency, U.S.E.P. (Ed.), *Air Quality Criteria for Ozone and Related Photochemical Oxidants* (2006 Final). Washington, DC.
- EPA, 2013. In: Agency, U.S.E.P. (Ed.), *Integrated Science Assessment of Ozone and Related Photochemical Oxidants* (Final Report). Washington, DC.
- Federal Register, 2007. Environmental Protection Agency, 40 CFR Parts 50 and 51, Treatment of Data Influenced by Exceptional Events; Final Rule, pp. 13560–13581.
- Federal Register, 2010. National Ambient Air Quality Standards for Ozone, pp. 2938–3052.
- Fiore, A.M., Dentener, F.J., Wild, O., Cuvelier, C., Schultz, M.G., Hess, P., Textor, C., Schulz, M., Doherty, R.M., Horowitz, L.W., MacKenzie, I.A., Sanderson, M.G., Shindell, D.T., Stevenson, D.S., Szopa, S., Van Dingenen, R., Zeng, G., Atherton, C., Bergmann, D., Bey, I., Carmichael, G., Collins, W.J., Duncan, B.N., Faluvegi, G., Folberth, G., Gauss, M., Gong, S., Hauglustaine, D., Holloway, T., Isaksen, I.S.A., Jacob, D.J., Jonson, J.E., Kaminski, J.W., Keating, T.J., Lupa, A., Marmer, E., Montanaro, V., Park, R.J., Pitari, G., Pringle, K.J., Pyle, J.A., Schroeder, S., Vivanco, M.G., Wind, P., Wojcik, G., Wu, S., Zuber, A., 2009. Multimodel estimates of intercontinental source-receptor relationships for ozone pollution. *J. Geophys. Res.* 114, D04301.
- Fiore, A.M., Horowitz, L.W., Purves, D.W., Levy II, H., Evans, M.J., Wang, Y., Li, Q., Yantosca, R.M., 2005. Evaluating the contribution of changes in isoprene emissions to surface ozone trends over the eastern United States. *J. Geophys. Res.* 110, D12303.
- Fiore, A.M., Jacob, D.J., Liu, H., Yantosca, R.M., Fairlie, T.D., Li, Q., 2003. Variability in surface ozone background over the United States: implications for air quality policy. *J. Geophys. Res.* 108, 4787.
- Fiore, A.M., Jacob, D.J., Bey, I., Yantosca, R.M., Field, B.D., Fusco, A.C., Wilkinson, J.G., 2002. Background ozone over the United States in summer: origin, trend, and contribution to pollution episodes. *J. Geophys. Res.* 107, 4275.
- Guenther, A., Karl, T., Harley, P., Wiedinmyer, C., Palmer, P., Geron, C., 2006. Estimates of global terrestrial isoprene emissions using MEGAN (Model of Emissions of Gases and Aerosols from Nature). *Atmos. Chem. Phys.* 6, 3181–3210.
- Hilsenrath, E., Chance, K., 2013. NASA ups the TEMPO on monitoring air pollution. *Earth Obs.* 25, 10–15, 35.
- Horowitz, L.W., Fiore, A.M., Milly, G.P., Cohen, R.C., Perring, A., Wooldridge, P.J., Hess, P.G., Emmons, L.K., Lamarque, J.-F., 2007. Observational constraints on the chemistry of isoprene nitrates over the eastern United States. *J. Geophys. Res.* 112, D12508.
- Horowitz, L.W., Walters, S., Mauzerall, D.L., Emmons, L.K., Rasch, P.J., Granier, C., Tie, X., Lamarque, J.-F., Schultz, M.G., Tyndall, G.S., Orlando, J.J., Brasseur, G.P., 2003. A global simulation of tropospheric ozone and related tracers: description and evaluation of MOZART, version 2. *J. Geophys. Res.* 108, 4784.
- Hudman, R.C., Jacob, D.J., Turquety, S., Leibensperger, E.M., Murray, L.T., Wu, S., Gilliland, A.B., Avery, M., Bertram, T.H., Brune, W., Cohen, R.C., Dibb, J.E., Flocke, F.M., Fried, A., Holloway, J., Neuman, J.A., Orville, R., Perring, A., Ren, X., Sachse, G.W., Singh, H.B., Swanson, A., Wooldridge, P.J., 2007. Surface and lightning sources of nitrogen oxides over the United States: magnitudes, chemical evolution, and outflow. *J. Geophys. Res.* 112, D12S05.
- Jacob, D.J., Horowitz, L.W., Munger, J.W., Heikes, B.G., Dickerson, R.R., Artz, R.S., Keene, W.C., 1995. Seasonal transition from NO_x- to hydrocarbon-limited conditions for ozone production over the eastern United States in September. *J. Geophys. Res.* 100, 9315–9324.
- Jaffe, D., 2011. Relationship between surface and free tropospheric ozone in the western U.S. *Environ. Sci. Technol.* 45, 432–438.
- Jaffe, D.A., Wigger, N.L., 2012. Ozone production from wildfires: a critical review. *Atmos. Environ.* 51, 1–10.
- Kalnay, E., Kanamitsu, M., Kistler, R., Collins, W., Deaven, D., Gandin, L., Iredell, M., Saha, S., White, C., Woollen, J., Zhu, Y., Leetmaa, A., Reynolds, R., Chelliah, M., Ebisuzaki, W., Higgins, W., Janowiak, J., Mo, K.C., Ropelewski, C., Wang, J., Jenne, R., Joseph, D., 1996. The NCEP/NCAR 40-Year reanalysis project. *Bull. Am. Meteorol. Soc.* 77, 437–471.
- Kaynak, B., Hu, Y., Martin, R.V., Russell, A.G., Choi, Y., Wang, Y., 2008. The effect of lightning NO_x production on surface ozone in the continental United States. *Atmos. Chem. Phys.* 8, 5151–5159.
- Lamarque, J.-F., Kyle, G., Meinshausen, M., Riahi, K., Smith, S., van Vuuren, D., Conley, A., Vitt, F., 2011. Global and regional evolution of short-lived radiatively active gases and aerosols in the representative concentration pathways. *Clim. Change* 109, 1–22.
- Lamarque, J.F., Bond, T.C., Eyring, V., Granier, C., Heil, A., Klimont, Z., Lee, D., Liousse, C., Mieville, A., Owen, B., Schultz, M.G., Shindell, D., Smith, S.J., Stehfest, E., Van Aardenne, J., Cooper, O.R., Kainuma, M., Mahowald, N., McConnell, J.R., Naik, V., Riahi, K., van Vuuren, D.P., 2010. Historical (1850–2000) gridded anthropogenic and biomass burning emissions of reactive gases and aerosols: methodology and application. *Atmos. Chem. Phys.* 10, 7017–7039.
- Langford, A.O., Aikin, K.C., Eubank, C.S., Williams, E.J., 2009. Stratospheric contribution to high surface ozone in Colorado during springtime. *Geophys. Res. Lett.* 36, L12801.
- Lin, M., Fiore, A.M., Cooper, O.R., Horowitz, L.W., Langford, A.O., Levy, H., Johnson, B.J., Naik, V., Oltmans, S.J., Senff, C.J., 2012a. Springtime high surface ozone events over the western United States: quantifying the role of stratospheric intrusions. *J. Geophys. Res. Atmos.* 117, D00V22.
- Lin, M., Fiore, A.M., Horowitz, L.W., Cooper, O.R., Naik, V., Holloway, J., Johnson, B.J., Middlebrook, A.M., Oltmans, S.J., Pollack, I.B., Ryerson, T.B., Warner, J.X., Wiedinmyer, C., Wilson, J., Wyman, B., 2012b. Transport of Asian ozone pollution into surface air over the western United States in spring. *J. Geophys. Res.* 117, D00V07.
- Lin, M., Horowitz, L.W., Oltmans, S.J., Fiore, A.M., Fan, S., 2014. Tropospheric ozone trends at Mauna Loa observatory tied to decadal climate variability. *Nat. Geosci.* 7, 136–143.
- Liu, X., Bhartia, P.K., Chance, K., Spurr, R.J.D., Kurosu, T.P., 2010. Ozone profile retrievals from the ozone monitoring instrument. *Atmos. Chem. Phys.* 10, 2521–2537.
- Mao, J., Paulot, F., Jacob, D.J., Cohen, R.C., Crounse, J.D., Wennberg, P.O., Keller, C.A., Hudman, R.C., Barkley, M.P., Horowitz, L.W., 2013. Ozone and organic nitrates over the eastern United States: sensitivity to isoprene chemistry. *J. Geophys. Res. Atmos.* 118, 1–13. <http://dx.doi.org/10.1002/jgrd.50817>.
- Martin, R.V., Sauvage, B., Folkens, I., Sioris, C.E., Boone, C., Bernath, P., Ziemke, J., 2007. Space-based constraints on the production of nitric oxide by lightning. *J. Geophys. Res.* 112, D09309.
- McDonald-Buller, E.C., Allen, D.T., Brown, N., Jacob, D.J., Jaffe, D., Kolb, C.E., Lefohn, A.S., Oltmans, S., Parrish, D.D., Yarwood, G., Zhang, L., 2011. Establishing policy relevant background (PRB) ozone concentrations in the United States. *Environ. Sci. Technol.* 45, 9484–9497.
- McKeen, S.A., Wotawa, G., Parrish, D.D., Holloway, J.S., Buhr, M.P., Hübler, G., Fehsenfeld, F.C., Meagher, J.F., 2002. Ozone production from Canadian wildfires during June and July of 1995. *J. Geophys. Res. Atmos.* 107, ACH 7-1-ACH 7-25.

- McLinden, C.A., Olsen, S.C., Hannegan, B., Wild, O., Prather, M.J., Sundet, J., 2000. Stratospheric ozone in 3-D models: a simple chemistry and the cross-tropopause flux. *J. Geophys. Res.* 105, 14653–14665.
- Mickley, L.J., Jacob, D.J., Rind, D., 2001. Uncertainty in preindustrial abundance of tropospheric ozone: implications for radiative forcing calculations. *J. Geophys. Res.* 106, 3389–3399.
- Mueller, S.F., Mallard, J.W., 2011. Contributions of natural emissions to ozone and PM_{2.5} as simulated by the community multiscale air quality (CMAQ) model. *Environ. Sci. Technol.* 45, 4817–4823.
- Murray, L.T., Jacob, D.J., Logan, J.A., Hudman, R.C., Koshak, W.J., 2012. Optimized regional and interannual variability of lightning in a global chemical transport model constrained by LIS/OTD satellite data. *J. Geophys. Res. Atmos.* 117, D20307.
- Naik, V., Horowitz, L.W., Fiore, A.M., Ginoux, P., Mao, J., Aghedo, A.M., Levy, H., 2013. Impact of preindustrial to present-day changes in short-lived pollutant emissions on atmospheric composition and climate forcing. *J. Geophys. Res. Atmos.* 118, 8086–8110.
- Olivier, J.G.J., Berdowski, J.J.M., 2001. Global emissions sources and sinks. In: Berdowski, J., Guicherit, R., Heij, B.J. (Eds.), *The Climate System*. Lisse, The Netherlands, pp. 33–78.
- Park, R.J., Jacob, D.J., Field, B.D., Yantosca, R.M., Chin, M., 2004. Natural and trans-boundary pollution influences on sulfate-nitrate-ammonium aerosols in the United States: implications for policy. *J. Geophys. Res. Atmos.* 109, D15204.
- Parrella, J.P., Jacob, D.J., Liang, Q., Zhang, Y., Mickley, L.J., Miller, B., Evans, M.J., Yang, X., Pyle, J.A., Theys, N., Van Roozendaal, M., 2012. Tropospheric bromine chemistry: implications for present and pre-industrial ozone and mercury. *Atmos. Chem. Phys.* 12, 6723–6740.
- Perring, A.E., Bertram, T.H., Wooldridge, P.J., Fried, A., Heikes, B.G., Dibb, J., Crounse, J.D., Wennberg, P.O., Blake, N.J., Blake, D.R., Brune, W.H., Singh, H.B., Cohen, R.C., 2009. Airborne observations of total RONO₂: new constraints on the yield and lifetime of isoprene nitrates. *Atmos. Chem. Phys.* 9, 1451–1463.
- Prather, M.J., Zhu, X., Tang, Q., Hsu, J., Neu, J.L., 2011. An atmospheric chemist in search of the tropopause. *J. Geophys. Res.* 116, D04306.
- Price, C., Rind, D., 1992. A simple lightning parameterization for calculating global lightning distributions. *J. Geophys. Res. Atmos.* 97, 9919–9933.
- Rasmussen, D.J., Fiore, A.M., Naik, V., Horowitz, L.W., McGinnis, S.J., Schultz, M.G., 2012. Surface ozone-temperature relationships in the eastern US: a monthly climatology for evaluating chemistry-climate models. *Atmos. Environ.* 47, 142–153.
- Reid, N., Yap, D., Bloxam, R., 2008. The potential role of background ozone on current and emerging air issues: an overview. *Air Qual. Atmos. Health* 1, 19–29.
- Reidmiller, D.R., Fiore, A.M., Jaffe, D.A., Bergmann, D., Cuvelier, C., Dentener, F.J., Duncan, B.N., Folberth, G., Gauss, M., Gong, S., Hess, P., Jonson, J.E., Keating, T., Lupu, A., Marmer, E., Park, R., Schultz, M.G., Shindell, D.T., Szopa, S., Vivanco, M.G., Wild, O., Zuber, A., 2009. The influence of foreign vs. North American emissions on surface ozone in the US. *Atmos. Chem. Phys.* 9, 5027–5042.
- Singh, H.B., Anderson, B.E., Brune, W.H., Cai, C., Cohen, R.C., Crawford, J.H., Cubison, M.J., Czech, E.P., Emmons, L., Fuelberg, H.E., Huey, G., Jacob, D.J., Jimenez, J.L., Kadowela, A., Kondo, Y., Mao, J., Olson, J.R., Sachse, G.W., Vay, S.A., Weinheimer, A., Wennberg, P.O., Wisthaler, A., 2010. Pollution influences on atmospheric composition and chemistry at high northern latitudes: boreal and California forest fire emissions. *Atmos. Environ.* 44, 4553–4564.
- Task Force on Hemispheric Transport of Air Pollution (TFHTAP), 2010. Hemispheric transport of air pollution 2010 part A: ozone and particulate matter, air pollution studies No. 17. In: Dentener, F., Keating, T., Akimoto, H. (Eds.), *Air Pollution Studies No. 17*. United Nations, New York.
- van der Werf, G.R., Randerson, J.T., Giglio, L., Collatz, G.J., Kasibhatla, P.S., Arellano Jr., A.F., 2006. Interannual variability in global biomass burning emissions from 1997 to 2004. *Atmos. Chem. Phys.* 6, 3423–3441.
- Vingarzan, R., 2004. A review of surface ozone background levels and trends. *Atmos. Environ.* 38, 3431–3442.
- Wang, H., Jacob, D.J., Le Sager, P., Streets, D.G., Park, R.J., Gilliland, A.B., van Donkelaar, A., 2009. Surface ozone background in the United States: Canadian and Mexican pollution influences. *Atmos. Environ.* 43, 1310–1319.
- Wang, Y.X., McElroy, M.B., Jacob, D.J., Yantosca, R.M., 2004. A nested grid formulation for chemical transport over Asia: applications to CO. *J. Geophys. Res. Atmos.* 109, D22307.
- Wild, O., Fiore, A.M., Shindell, D.T., Doherty, R.M., Collins, W.J., Dentener, F.J., Schultz, M.G., Gong, S., MacKenzie, I.A., Zeng, G., Hess, P., Duncan, B.N., Bergmann, D.J., Szopa, S., Jonson, J.E., Keating, T.J., Zuber, A., 2012. Modelling future changes in surface ozone: a parameterized approach. *Atmos. Chem. Phys.* 12, 2037–2054.
- Wu, S., Mickley, L.J., Jacob, D.J., Rind, D., Streets, D.G., 2008. Effects of 2000–2050 changes in climate and emissions on global tropospheric ozone and the policy-relevant background surface ozone in the United States. *J. Geophys. Res.* 113, D18312.
- Zhang, L., Jacob, D.J., Boersma, K.F., Jaffe, D.A., Olson, J.R., Bowman, K.W., Worden, J.R., Thompson, A.M., Avery, M.A., Cohen, R.C., Dibb, J.E., Flocke, F.M., Fuelberg, H.E., Huey, L.G., McMillan, W.W., Singh, H.B., Weinheimer, A.J., 2008. Transpacific transport of ozone pollution and the effect of recent Asian emission increases on air quality in North America: an integrated analysis using satellite, aircraft, ozonesonde, and surface observations. *Atmos. Chem. Phys.* 8, 6117–6136.
- Zhang, L., Jacob, D.J., Downey, N.V., Wood, D.A., Blewitt, D., Carouge, C.C., van Donkelaar, A., Jones, D.B.A., Murray, L.T., Wang, Y., 2011. Improved estimate of the policy-relevant background ozone in the United States using the GEOS-Chem global model with $\frac{1}{2}^\circ \times \frac{2}{3}^\circ$ horizontal resolution over North America. *Atmos. Environ.* 45, 6769–6776.
- Zhang, L., Jacob, D.J., Liu, X., Logan, J.A., Chance, K., Eldering, A., Bojkov, B.R., 2010. Intercomparison methods for satellite measurements of atmospheric composition: application to tropospheric ozone from TES and OMI. *Atmos. Chem. Phys.* 10, 4725–4739.
- Zhang, L., Jacob, D.J., Yue, X., Downey, N.V., Wood, D.A., Blewitt, D., 2014. Sources contributing to background surface ozone in the US Intermountain West. *Atmos. Chem. Phys.* 14, 5295–5309. <http://dx.doi.org/10.5194/acp-14-5295-2014>.